Superconducting Cavities

Jacek Sekutowicz
DESY

Lecture I

1. Introduction and History
2. RF Parameters
3. Criteria for Cavity Design
4. Test Results of single-cell cavities

Lecture II

5. Multi-cell Structures and Weakly Coupled Structures
6. Tools for RF-design
7. LEC and Transient state
8. Performance test
9. Mechanical Design

Milestones that led to accelerators based on SRF

Superconductivity

1908: Heike Kamerlingh Onnes (Holland)
Liquefied Helium for the first time.

1911: Heike Kamerlingh Onnes
Discovered Superconductivity.

1928-34: Walther Meissner (Germany)
Discovered Superconductivity of Ta, V, Ti and Nb.

RF Acceleration

1924: Gustaf Ising (Sweden)
The First Publication on RF Acceleration, Arkiv för Matematik, Astronomi och Fysik,

1928: Rolf Wideröe (Norway, Germany)
Built the first RF Accelerator, Arch. für Elektrotechnik 21, vol.18.

1947: Luis Alvarez (USA)
Built first DTL (32 MeV protons).

1947: W. Hansen (USA)
Built first 6 MeV e-accelerator, Mark I (TW- structure).

Superconductivity RF Acceleration

1961: W. Fairbank (Stanford Univ.)
Presented the first proposal for a superconducting accelerator

1964: W. Fairbank, A. Schwettman, P. Wilson (Stanford Univ.)
First acceleration of electrons with sc lead cavity

1970: J. Turneaure (Stanford Univ.)
E_{peak} =70 MV/m and Q~10^{10} in 8.5 GHz cavity !

1968-1981: M. McAshan, A. Schwettman, T. Smith, J. Turneaure, P. Wilson (Stanford Univ.)

Developed and Constructed the Superconducting Accelerator SCA

Since then, we have built many sc accelerators and we are constructing and making plans for many new facilities.

Dismantled Facilities

1. TRISTAN (32/49m)*
2. LEP (288/490m)
3. HERA (16/19m)

*(Number of cavities / total active length)

Operating Facilities

1. SCA (4/28m)
2. S-DALINAC (10/10m)
3. CESR (4/1.2 m)
4. CEBAF (320/160m)
5. KEK B-Factory (8/2.4m)
6. Taiwan LS (1+1/0.3m)
7. Canadian LS (1+1/0.3m)
8. DIAMOND (3/0.9m)
9. SOLEIL (4/1.7m)
10. TTF II (56/58m)
11. SNS (81/65m)
12. JLab-FEL (24/14m)
13. LHC (16/6m)
14. ELBE (6/6m)

Tomorrow Facilities		Day after Tomorrow Facilities	
1. CEBAF-12GeV	(400/216m)	1. FRIB	(non-elliptical 47/~70m)
2. SNS-upgrade	(117/ 98m)	2. X-Ray MIT	(option 176 / 184m)
3. XFEL	(648/674m)	3. Project X	(elliptical 352 /~360m)
4. ERL-Cornell	(310/250m)	4. ERHIC………	
5. RHIC-cooling	(1/1 m)	5. ELIC …..	
6. BEPC II	(2/0.6m)	6. ILC …..	(~15764 /~16395m)
7. …………….			

ILC (~15764/~16395m)

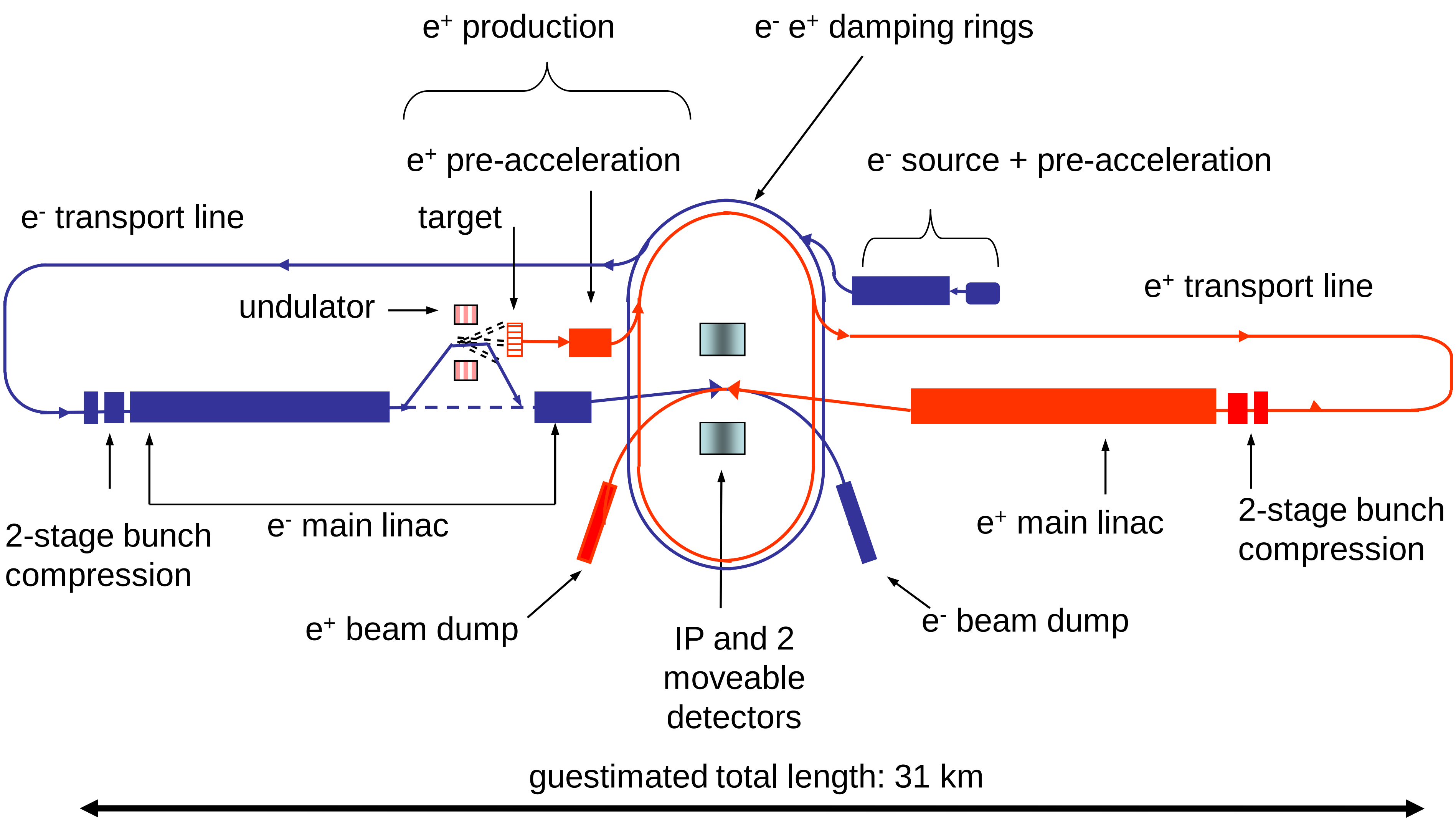

The “heart” of all mentioned facilities are (were) sc standing wave accelerating structures, here elliptical with ß ≥ 0.61.

FERMI 3.9 GHz

TESLA/ILC 1.3 GHz

LEP 0.352 GHz

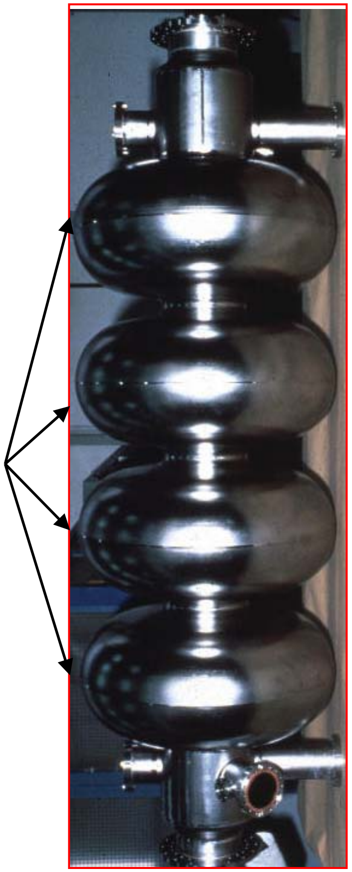

cells

S-DALINAC 3 GHz

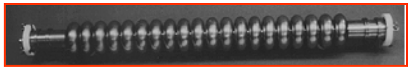

SNS ß=0.61,0.81, 0.805 GHz

CESR/CEBAF 1.5 GHz

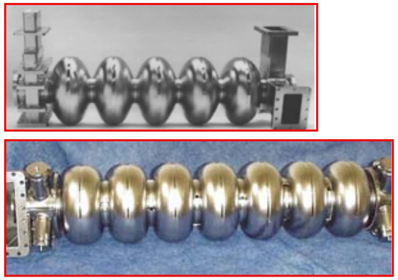

HERA 0.5 GHz

HEPL 1.3 GHz

KEK-B 0.5 GHz

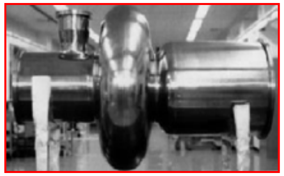

CESR 0.5 GHz

We have also many “heavy” particles accelerators based on low-ß sc cavities.
You had lecture on this topic by Dr. Maurizio Vretenar on Friday.
The low-ß cavities are not discussed in this lecture.

Accelerator/Upgrade/Project

- ISAC-II
- SPIRAL-II
- SARAF
- IUAC
- HIE-REX
- EURISOL
- SPES
- LNL
- ReA3
- FRIB
- IFMIF

QWR

HWR

Spoke

What was the progress in the 33 years and what do we need in the next 10 years?

~ 28 m long SCA at Stanford, 1977.

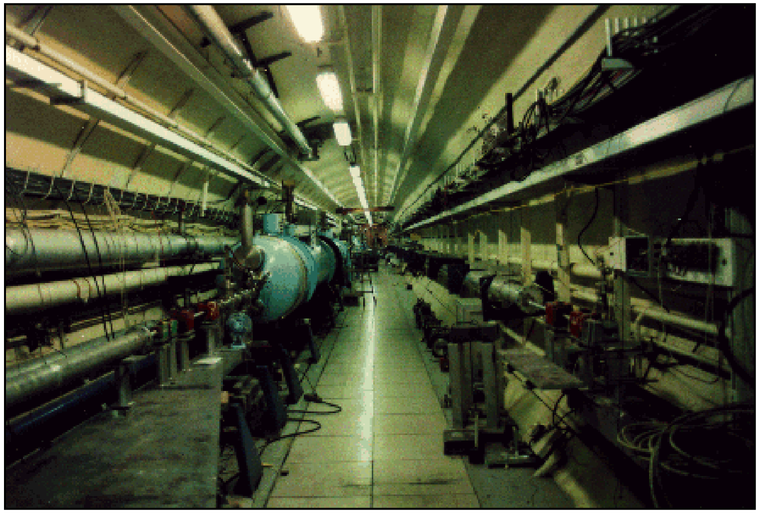

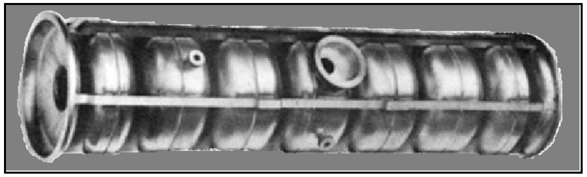

E_{acc} ~2 (2.5) MV/m in cw (10% DF).
4 Structures 5.65m + capture + pre-accelerator.

~ 21.6 km long ILC linac, 2018+

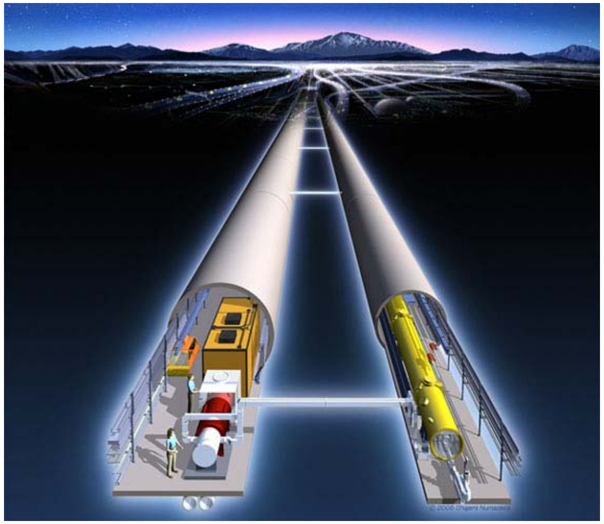

E_{acc} > 34 MV/m shown in several 9-cells in the cw test.

⬇

This gradient is required in all 15764 cavities.

Results at DESY (status 2010):

cw test result at 2 K for 8 best electropolished 9-cell TESLA cavities.

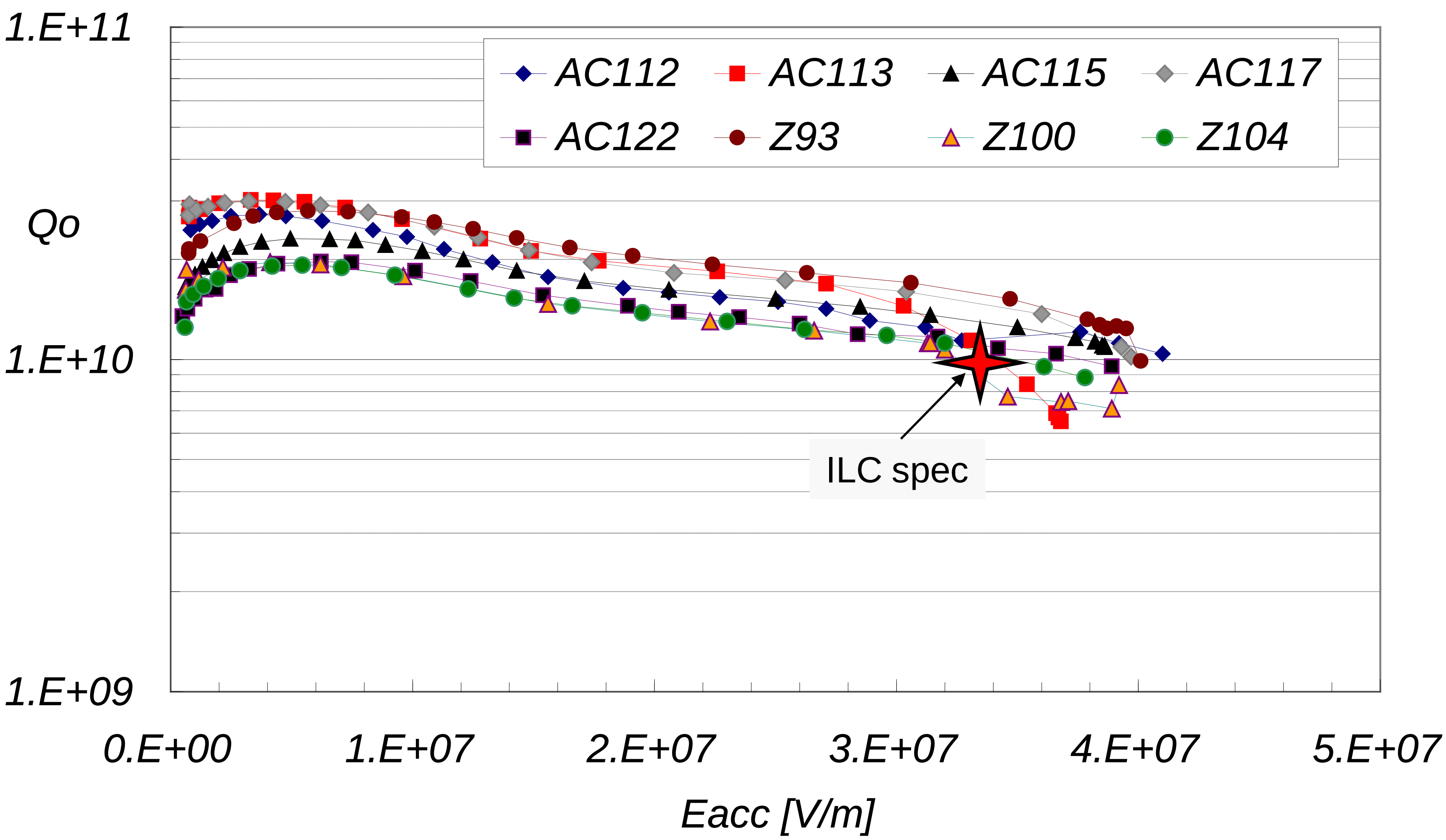

2.1. Cavities and their Eigenmodes *(the simplest example)*

Cavity ≡ a volume, partially closed by the metal wall, capable to store the E-H energy

First assumption:

1. Stored E-H fields **are harmonic** in time.

Maxwell equations for the harmonic,
lossless case with no free charge in the volume

$$\begin{cases} \nabla \times H = i\omega\varepsilon E \\ \nabla \times E = -i\omega\mu H \\ \nabla \cdot E = 0 \\ \nabla \cdot H = 0 \end{cases}$$

Second assumption (good approximation for the elliptical cavities):

2. The volume is **cylindrically symmetric**. We commonly use the (r, φ, z) coordinates.

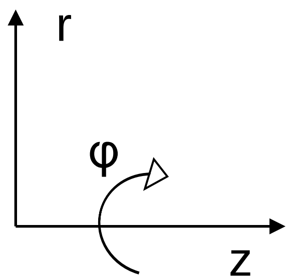

z is conventional direction of the acceleration and it is symmetry axis

$$\begin{cases} \nabla_c \times H = i\omega\varepsilon E \\ \nabla_c \times E = -i\omega\mu H \\ \nabla_c \cdot E = 0 \\ \nabla_c \cdot H = 0 \end{cases}$$

$$\nabla_c \times A = \vec{i}_r \left(\frac{1}{r}\frac{\partial A_z}{\partial \varphi} - \frac{\partial A_\varphi}{\partial z} \right) + \vec{i}_\varphi \left(\frac{\partial A_r}{\partial z} - \frac{\partial A_z}{\partial r} \right) + \vec{i}_z \left(\frac{1}{r}\frac{\partial (rA_\varphi)}{\partial r} - \frac{1}{r}\frac{\partial A_r}{\partial \varphi} \right)$$

$$\nabla_c \cdot A = \frac{1}{r}\frac{\partial (rA_r)}{\partial r} + \frac{1}{r}\frac{\partial A_\varphi}{\partial \varphi} + \frac{\partial A_z}{\partial z}$$

Third assumption

3. For the **acceleration** are suitable modes with **strong E** along the beam **trajectory**.

This ensures, by the proper phasing, maximal energy exchange between the cavity and beam.

<u>TM0xx-like monopole</u> modes have "very strong" E_z component on the symmetry axis.

Fields of the monopole modes do not depend on φ.

$$\frac{\partial E}{\partial \varphi} = 0 \qquad \frac{\partial H}{\partial \varphi} = 0$$

<u>Non monopole modes (HOM)</u> have component $E_z = 0$ on the symmetry axis.

Their fields dependent on φ.

Maxwell equations + boundary conditions for E and H lead to the <u>Helmholtz</u> equation, which is an eigenvalue problem.

For *H(r,z)* field of a monopole mode the equation is:

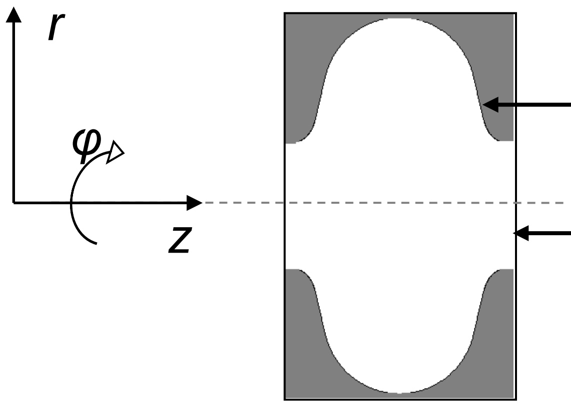

$$(\nabla_c^2 + \omega^2 \varepsilon\mu)H = 0$$

$n \cdot H = 0$ on metal wall

$\begin{cases} H = 0 \\ n \cdot H = 0 \end{cases}$ optionally on non metal boundary

$$\nabla_c^2 A = \nabla_c(\nabla_c \cdot A) - \nabla_c \times \nabla_c \times A$$

There is infinity number of TM0xx solutions (modes) to the Helmholtz equation.

All modes are determine by:

$$H_n(r,z)=[0,\ H_{\varphi,n}(r,z),0],$$
$$E_n(r,z)=[E_{r,n}(r,z),0,\ E_{z,n}(r,z)]$$

and by frequency ω_n .

2.2 What are figures of merit for a cavity storing E-H energy?

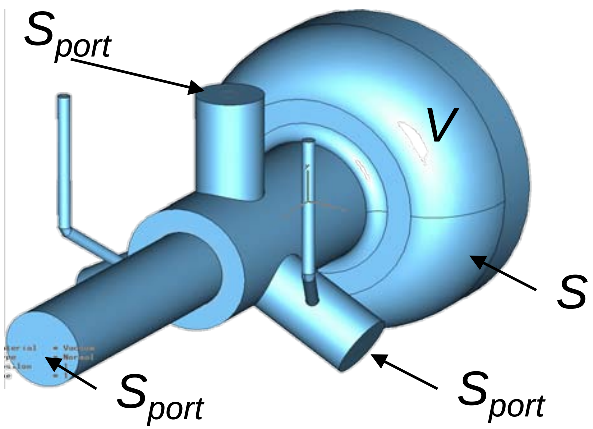

$W_n \equiv$ *stored energy of a mode n :* $\{\omega_n, E_n, H_n\}$.

$$W_n \equiv 2\mu \int_V \frac{H_n^2}{4} dV = 2\varepsilon \int_V \frac{E_n^2}{4} dV$$

Quality Factors

The measure of the energy loss in metal wall and due to the radiation via open ports:

Intrinsic $Q \equiv Qo$

$$Q_{0,n} \equiv \frac{\omega_n \cdot W_n}{P_n} = \frac{\omega_n \cdot W_n}{\frac{R_{s,n}}{2} \int_S H_n^2 ds}$$

External $Q \equiv Q_{ext}$

$$Q_{ext,n} \equiv \frac{\omega_n \cdot W_n}{P_{rad,n}} = \frac{\omega_n \cdot W_n}{\frac{1}{2} \int_{S_{port}} E_n \times H_n ds}$$

Geometric Factor

The measure of the energy loss in the metal wall for the surface resistance $R_{s,n}$=1Ω

$$G_n \equiv Q_{0,n} \cdot R_{s,n} = \frac{\omega_n \cdot W_n \cdot R_{s,n}}{P_n} = \frac{\omega_n \cdot W_n}{\frac{1}{2}\int_S H_n^2 ds}$$

It is the ratio of stored energy to the integral of $(H_n)^2$ on metal wall S.

2.3 What are figures of merit for the beam-cavity interaction?

This interaction which is:

- Acceleration
- Deceleration (ERL)
- HOMs excitation

can be described in the Frequency Domain (FD) or/and in Time Domain (TD).

$(R/Q)_n$; *beam impedance*

It is a "measure" of the energy exchange between point charge and mode n (FD).

Mode n : $\{\omega_n, E_n, H_n\}$.

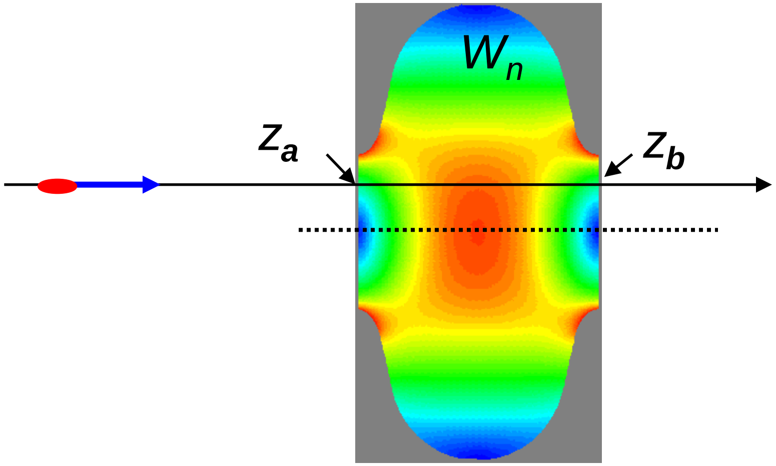

Trajectory of the point charge q, assumed here is a straight line.

$$V_n = \sqrt{\left(\int_{z_a}^{z_b} E_{n,z} \sin\left(\frac{\omega_n}{\beta c}(z - z_a)\right)dz\right)^2 + \left(\int_{z_a}^{z_b} E_{n,z} \cos\left(\frac{\omega_n}{\beta c}(z - z_a)\right)dz\right)^2}$$

$$(R/Q)_n \equiv \frac{V_n^2}{\omega_n W_n}$$

Longitudinal and Transverse Loss Factors (TD)
(Excitation of cavity modes)

Ultra relativistic point charge *q* passes empty cavity

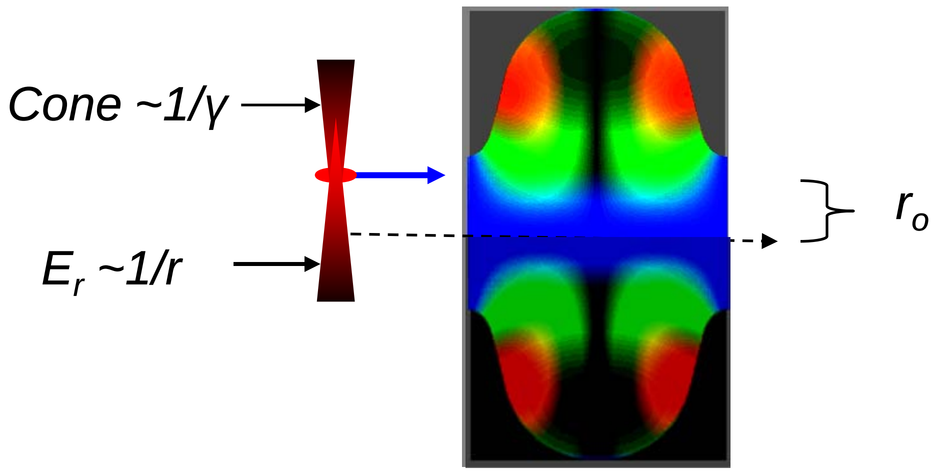

a. Density of the inducted charge on the wall depends on the distance to beam trajectory

b. The non uniform charge density on the metal wall causes the current flow on surface

The amount of energy lost by charge q to the cavity is:

$\Delta U_q = k_{\|} \cdot q^2$ for monopole modes (max. on axis)

$\Delta U_q = k_{\perp} \cdot q^2$ for non monopole modes (off axis)

where $k_{\|}$ and $k_{\perp}(r)$ are the loss factors for monopole and transverse modes respectively

The induced E-H field (wake) is a superposition of all cavity eigenmodes having the $E_n(r,\varphi,z)$ field along the particle trajectory.

Both description methods FD and TD are equivalent.

For an individual mode n and point-like charge:

$$k^{\mathbf{p}}_{\|,n} = \frac{\omega_n \cdot (R/Q)_n}{4}$$

Note the linac convention for (R/Q) definition.

Similar for other loss factors…….

2.4. Some “practical” RF parameters of the accelerating mode

At stored energy W_{acc} the mean value of the accelerating gradient is:

$$E_{acc} = \frac{\sqrt{\omega_{acc} \cdot W_{acc} \cdot (R/Q)_{acc}}}{l_{active}}$$

E_{peak} on the wall

B_{peak} on the wall

$$\boxed{\frac{E_{peak}}{E_{acc}}}$$

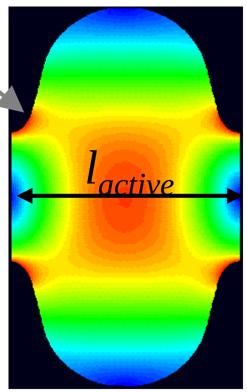

Contour plot of /E/

$$\boxed{\frac{B_{peak}}{E_{acc}}}$$

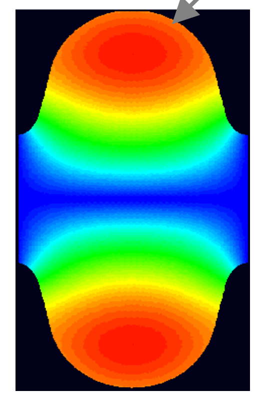

Contour plot of /B/

The ratio shows sensitivity of the shape to the field electron emission phenomenon.

The ratio shows limit in E_{acc} due to the break-down of superconductivity (Nb ~190 mT).

$$\boxed{G_{acc} \cdot (R/Q)_{acc}}$$

For the accelerating mode we often use the product: $G_{acc} \cdot (R/Q)_{acc}$, as a "measure" of the power P dissipated in the wall at given accelerating voltage V_{acc} and given surface resistance R_s.

$$\frac{P_{dissipated}}{V_{acc}^2} \equiv \frac{R_s}{\underbrace{G_{acc} \cdot (R/Q)_{acc}}}$$

Big improvements are possible:

- Due to superconductivity
- Due to the surface quality.

This is due to the geometry of cells

Moderate improvement possible.

cell-to-cell coupling k_{cc}

The k_{cc} is relevant for the accelerating mode passband of multi-cell structures

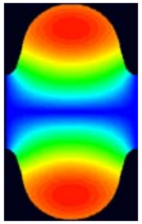

Single-cell structures are attractive because:

- It is easier to manage HOM damping
- There is no field flatness problem.
- Input coupler transfers less power
- They are easy for cleaning and preparation
- But it is expensive to base even a small linear accelerator on the single cells. We do it only for very high beam current machines.

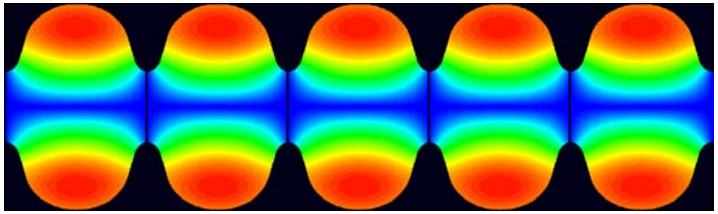

- Multi-cell structures are less expensive/m and allow for higher real-estate gradient.

Resonators closed by metal wall:

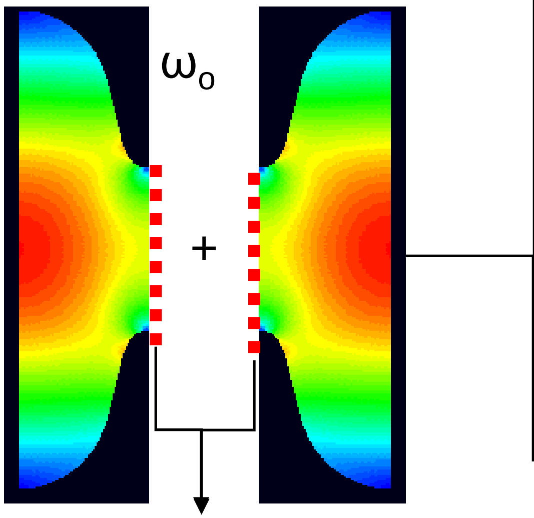

Symmetry planes for the H field

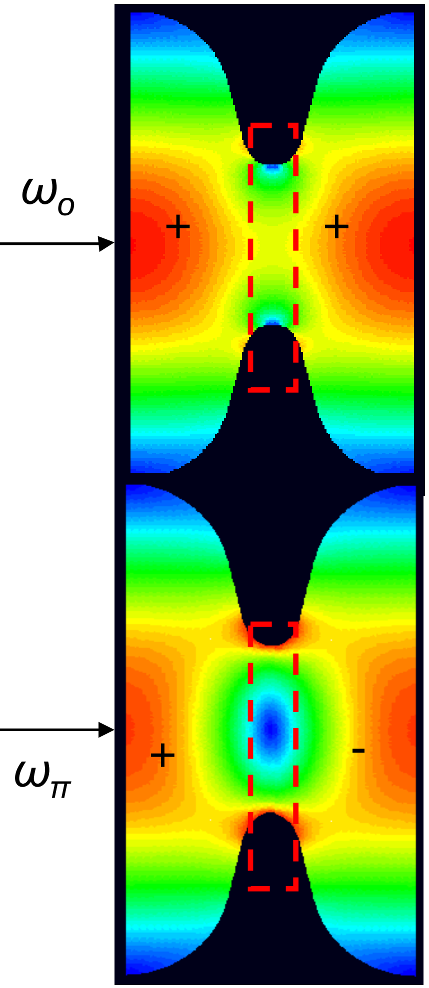

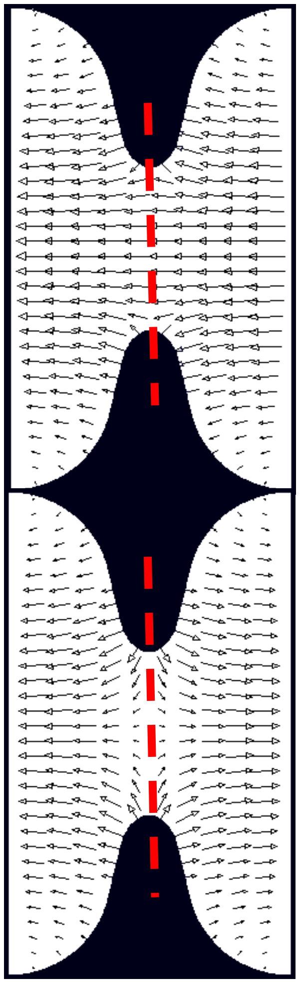

Symmetry plane for the H field

Symmetry plane for the E field,

which is an additional solution

The energy flux across the coupling region, refilling energy loss is proportional to the transverse components: H_φ and E_r

ω_o

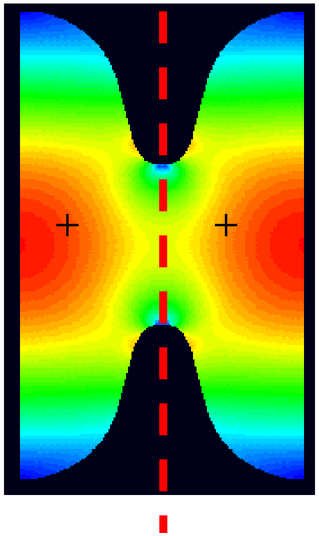

ω_π

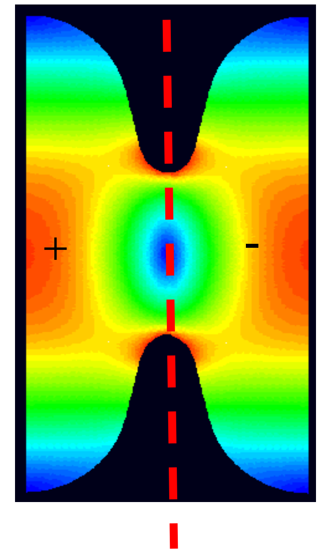

Small E_r (due to the losses) + strong H_φ at the symmetry plane

Small H_φ (due to the losses) + strong E_r at the symmetry plane

The normalized difference between these frequencies is a measure of the energy flow via the coupling region

$$k_{cc} = \frac{\omega_\pi - \omega_0}{\dfrac{\omega_\pi + \omega_0}{2}}$$

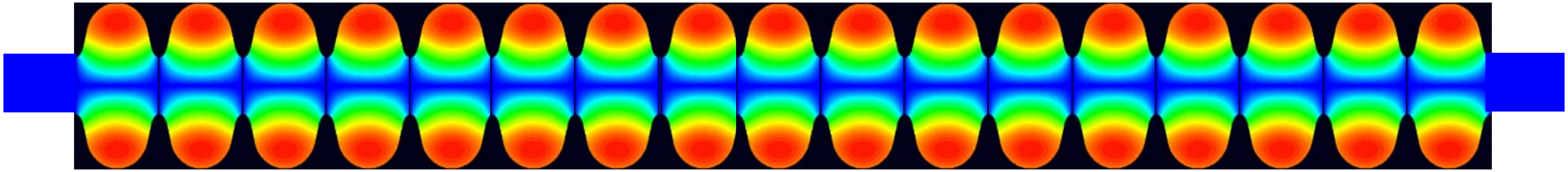

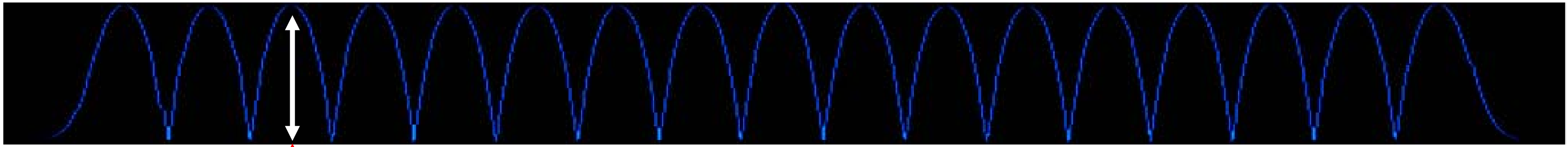

$$\frac{\Delta A_i}{A_i} = a_{ff} \frac{\Delta f_i}{f_i}$$

Field flatness factor a_{ff} for structure made of N cells and their coupling factor k_{cc}

$$a_{ff} = \frac{N^2}{k_{cc}}$$

The above formulae estimate the sensitivity of a multi-cell field profile to frequency errors of an individual cell for the accelerating mode (π-mode)

Criteria for inner cell design

We will discuss here design of inner cells because they “dominate” the RF properties of multi-cell superconducting accelerating structures.

RF parameters summary:

$FM \quad : \quad (R/Q), \;\; G, \;\; E_{peak}/E_{acc}, \;\; B_{peak}/E_{acc}, \;\; k_{cc}$

$HOM : \quad k_{\perp}, k_{\parallel}.$

There are 7 parameters we want to optimize for an inner cell.

Geometry :

iris ellipsis : *half-axis* h_r, h_z

iris radius : r_i

equator ellipsis : *half-axis* h_r, h_z

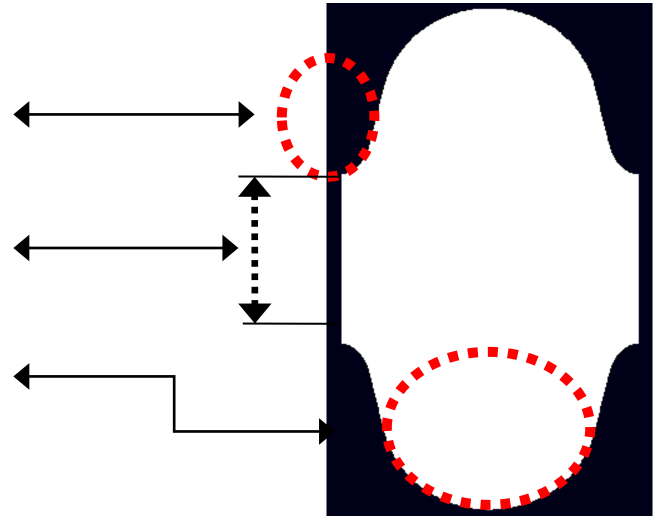

There is some kind of conflict <u>*7 parameters*</u> and only <u>*5 variables*</u> to “tune”

3. Criteria for Cavity Design

Criteria	*RF-parameter*	*Improves when*	*Cavity examples*
Operation at high gradient	E_{peak}/E_{acc}, B_{peak}/E_{acc} $\downarrow$	r_i $\downarrow$ *Iris & Equator shape*	*TESLA, HG CEBAF-12 GeV*
Low cryogenic losses	$(R/Q)\cdot G$ $\uparrow$	r_i $\downarrow$ *Equator shape*	*LL CEBAF-12 GeV*
High $I_{beam} \leftrightarrow$ *Low HOM impedance*	$k_{\perp}, k_{\parallel}$ $\downarrow$	r_i $\uparrow$	*B-Factory RHIC cooling*

We see here that r_i is a very "powerful variable" to trim the RF-parameters of a cavity.

Why for a smaller aperture (r_i)

- *(R/Q)* is bigger
- E_{peak}/E_{acc} , B_{peak}/E_{acc} are lower ?

E_{acc} is higher at the same stored energy in the cell with smaller aperture.

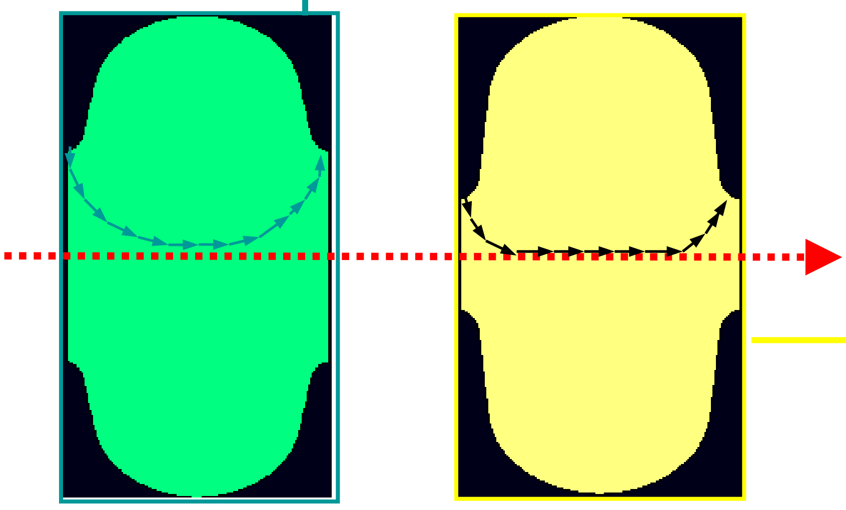

$r_i = 40$ mm $r_i = 20$ mm

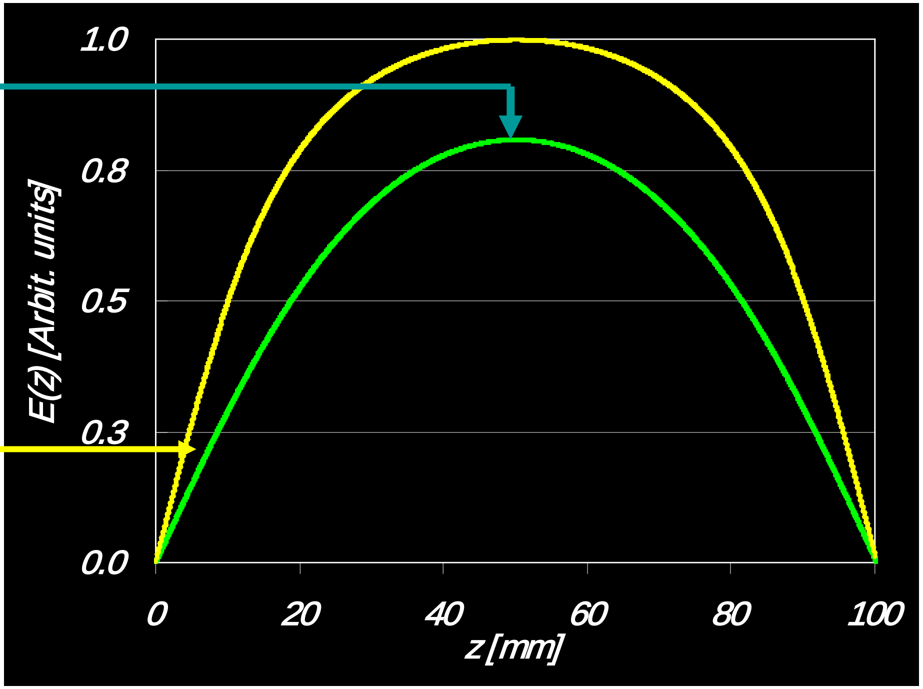

E_z *(z)* for small and big iris radius

Example:

{ (R/Q), E_{peak}/E_{acc} , B_{peak}/E_{acc} } vs. r_i for cell at _f = 1.5 GHz

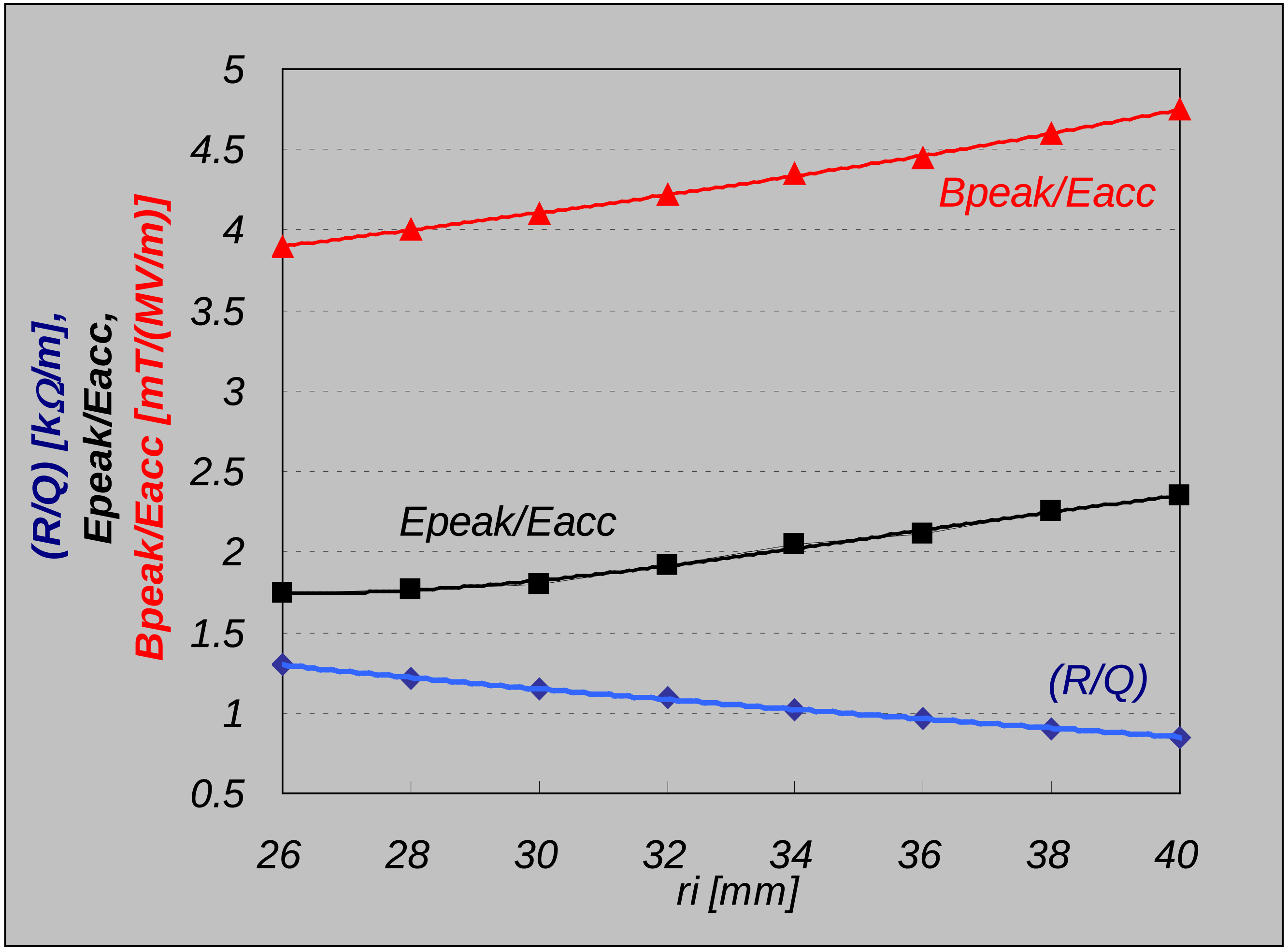

A. Mosnier, E. Haebel, SRF Workshop 1991

In addition to the iris radius r_i:

- B_{peak}/E_{acc} (and G) changes vs. the equator shape

1 Joule

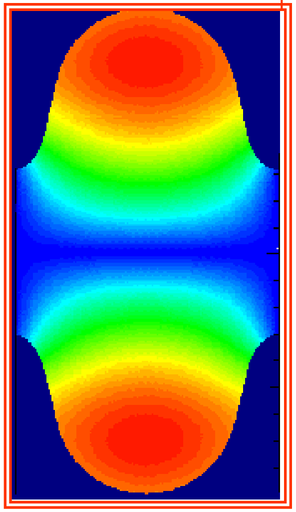

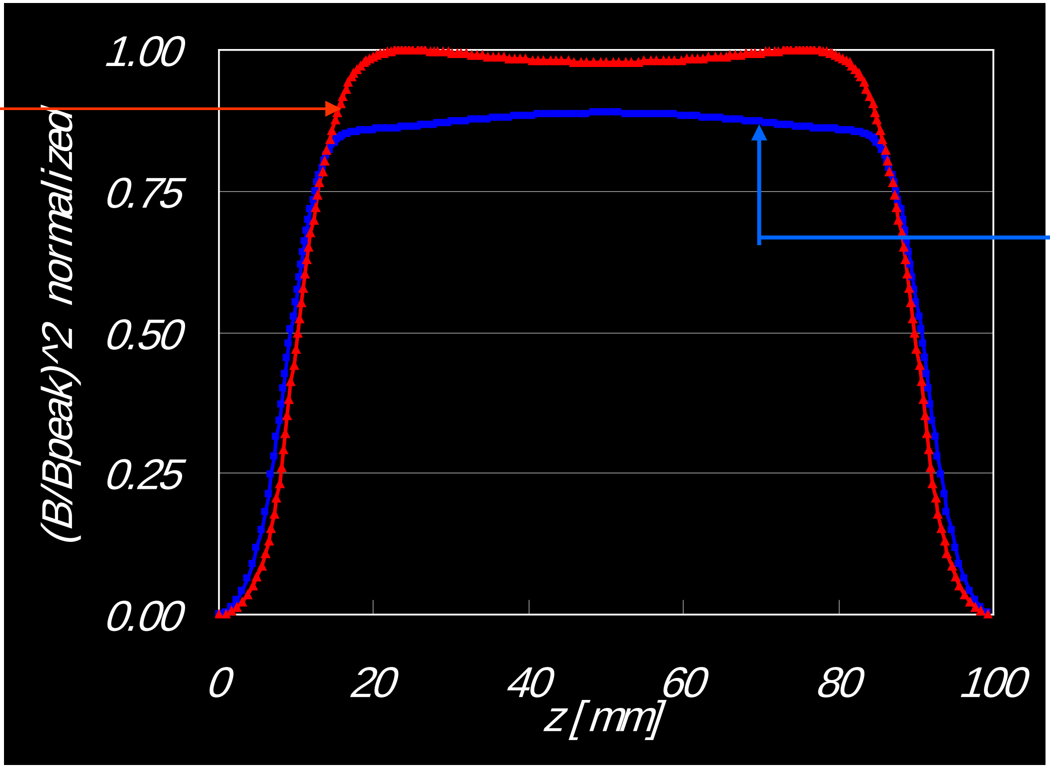

1 Joule

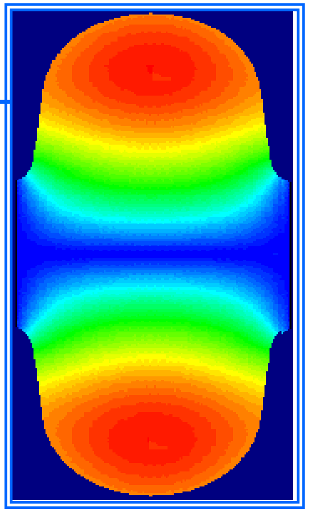

Similarly : E_{peak}/E_{acc} changes vs. the iris shape

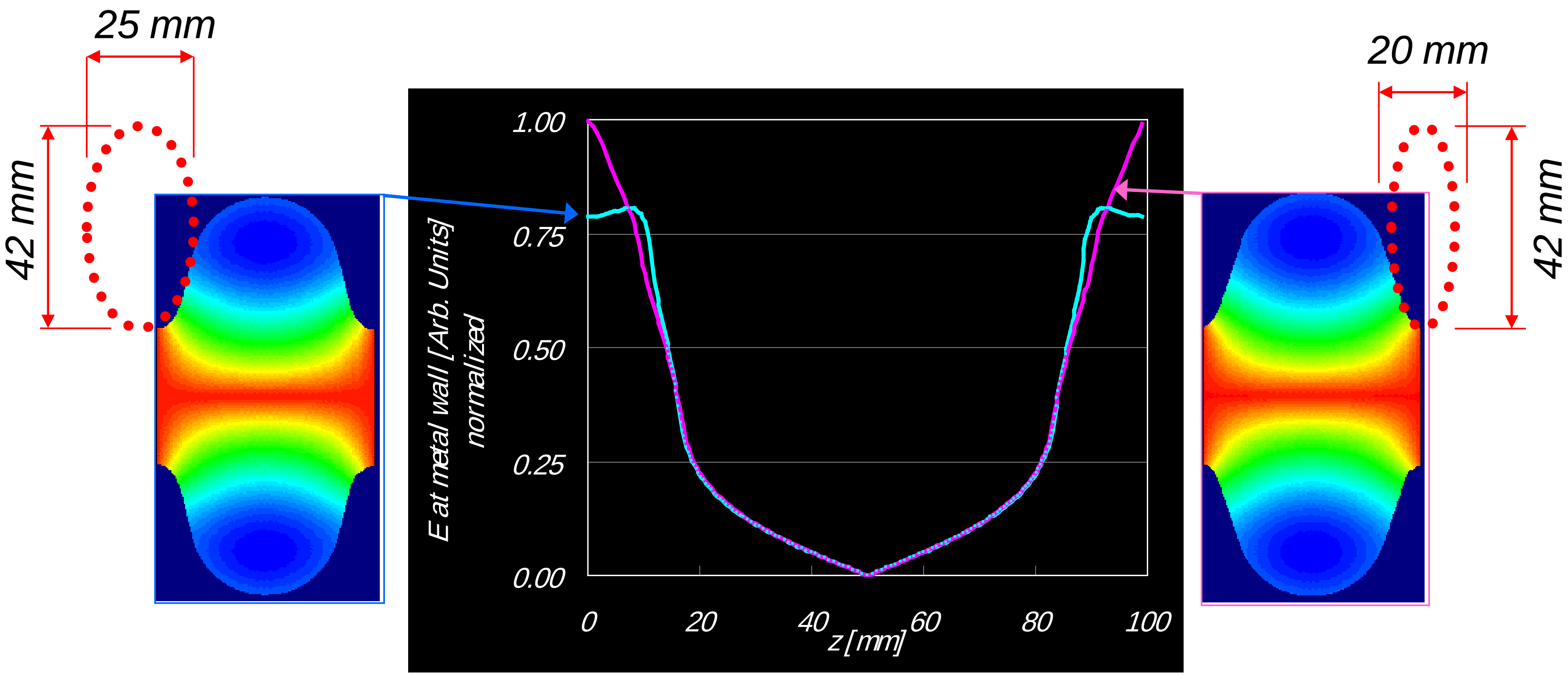

Both cells have the same: *f*, *(R/Q)* and r_i

We know that a smaller aperture r_i makes FM :

- *(R/Q)* higher
- B_{peak}/E_{acc} , E_{peak}/E_{acc} lower

$\Big\}$ (+)

but unfortunately a smaller aperture r_i makes:

- HOMs impedances ($k_\perp$, $k_\parallel$) higher
- cell-to-cell coupling (k_{cc}) weaker

$\Big\}$ (-)

HOMs loss factors ($k_\perp$, $k_\parallel$)

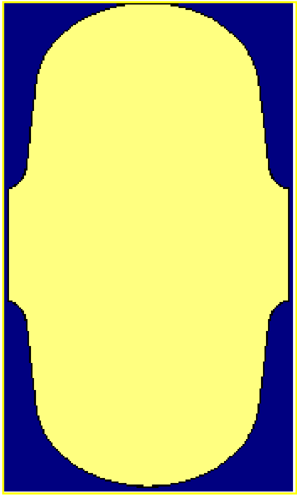

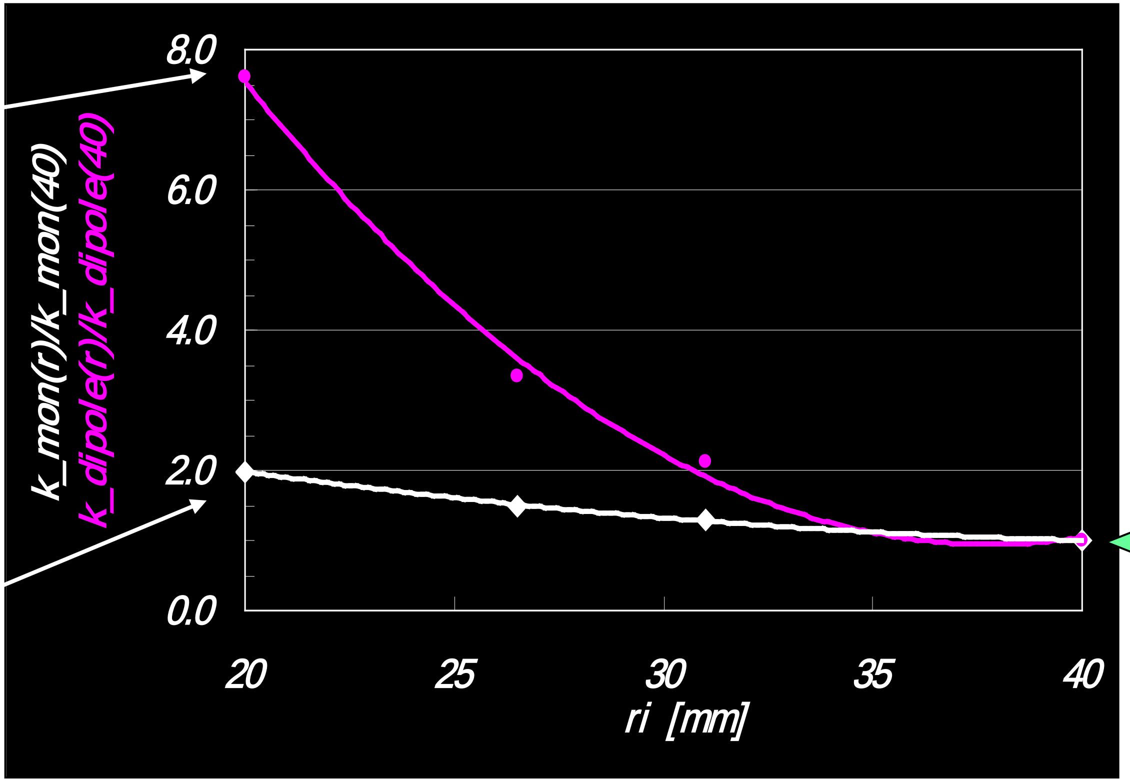

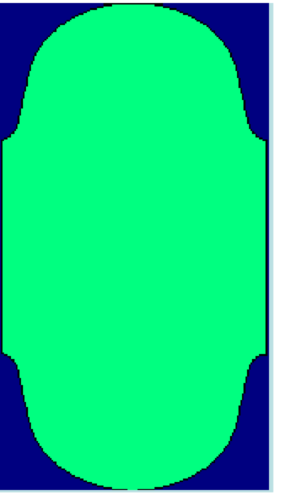

(R/Q) = *152* Ω

B_{peak}/E_{acc} = *3.5 mT/(MV/m)*

E_{peak}/E_{acc} = *1.9*

(R/Q) = *86* Ω

B_{peak}/E_{acc} = *4.6 mT/(MV/m)*

E_{peak}/E_{acc} = *3.2*

Cell-to-cell coupling, k_{cc}

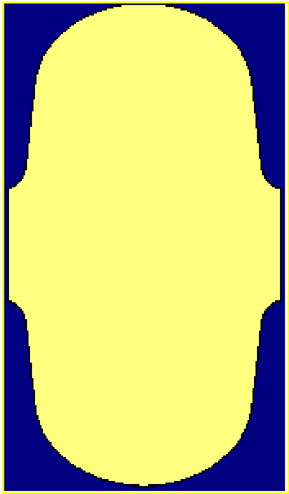

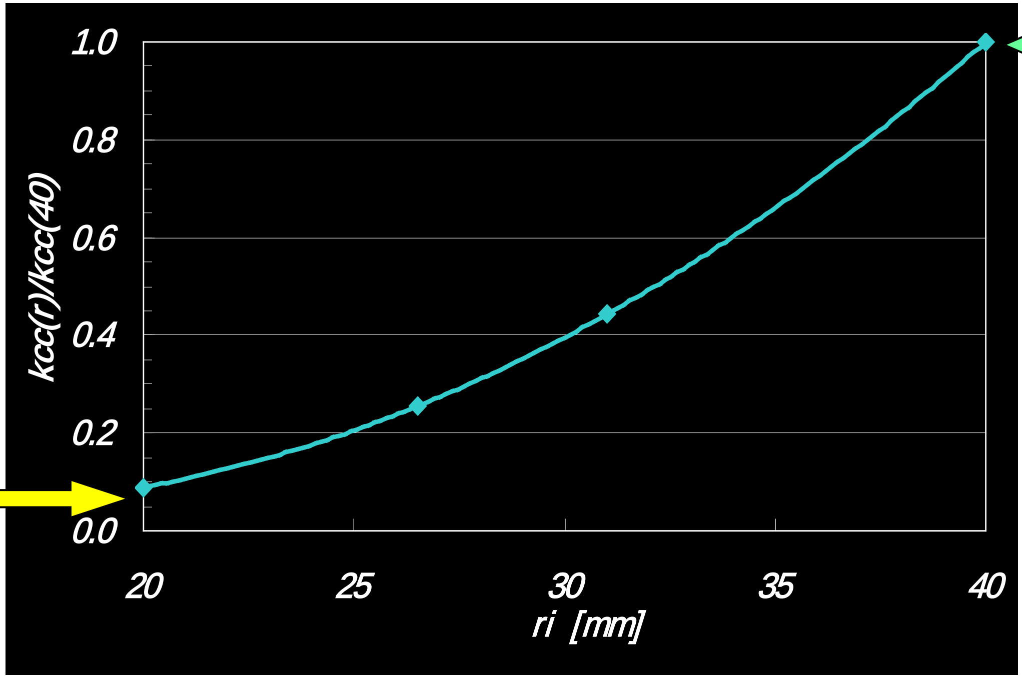

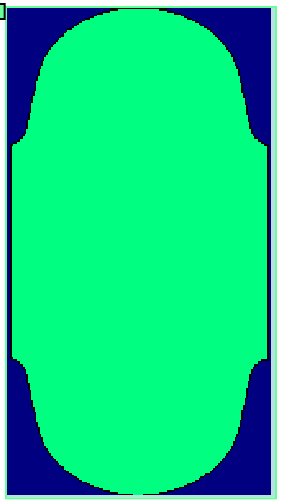

$(R/Q) = 152\ \Omega$

$B_{peak}/E_{acc} = 3.5\ mT/(MV/m)$

$E_{peak}/E_{acc} = 1.9$

$(R/Q) = 86\ \Omega$

$B_{peak}/E_{acc} = 4.6\ mT/(MV/m)$

$E_{peak}/E_{acc} = 3.2$

Frequency of the accelerating mode frequency

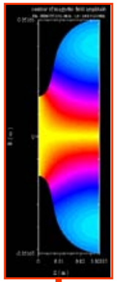

x 2 =

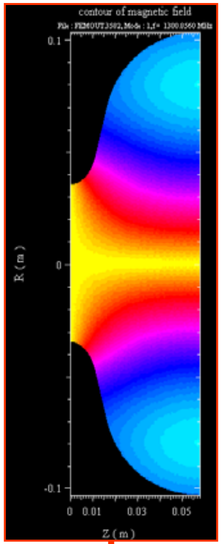

f_{π}	[MHz]	2600
R/Q	[Ω]	57
r/q=(R/Q)/l	[Ω/m]	2000
G	[Ω]	271

f_{π}	[MHz]	1300
R/Q	[Ω]	57
r/q=(R/Q)/l	[Ω/m]	1000
G	[Ω]	271

$$r/q=(R/Q)/l \sim f$$

From the formula, we learned before, one obtains:

$$P_{dissipated} = \frac{R_s \cdot V_{acc}^2}{G_{acc} \cdot (r/q)_{acc} \cdot l_{active}}$$

Higher f_π would be a good choice to minimize dissipation in the metal wall when the length l_{active} and final energy V_{acc} are fixed.

Unfortunately this applies only to room temperature structures made of Cu, which $R_s \sim (f)^{1/2}$.

For superconductors, like Nb:

$$R_s(f) = R_{res} + R_{BCS} = R_{res} + 0.0002 \cdot \frac{1}{T} \cdot \left(\frac{f[GHz]}{1.5}\right)^2 \cdot \exp\left(-\frac{17.67}{T}\right)$$

and R_s , which is $\sim (f)^2$ for higher f must be compensated with lower temperature T.

This is why ILC, XFEL, ERL,… (1.3GHz) will operate at 2 K (1.8 K), and

HERA (0.5 GHz) and LEP (0.352 GHz) could operate at 4.2 K

Examples of inner cells

		CEBAF Original Cornell ß=1	CEBAF -12 Low Loss ß=1	TESLA ß=1	SNS ß=0.61	SNS ß=0.81	RHIC Cooler ß=1
f_π	[MHz]	1497.0	1497.0	1300.0	805.0	805.0	703.7
k_{cc}	[%]	3.29	1.49	1.9	1.52	1.52	2.94
E_{peak}/E_{acc}	-	2.56	2.17	1.98	2.66	2.14	1.98
B_{peak}/E_{acc}	[mT/(MV/m)]	4.56	3.74	4.15	5.44	4.58	5.78
R/Q	[Ω]	96.5	128.8	113.8	49.2	83.8	80.2
G	[Ω]	273.8	280	271	176	226	225
R/Q*G	[Ω*Ω]	26421	36064	30840	8659	18939	18045
$k_\perp$ (σ_z=1mm)	[V/pC/cm^2]	0.22	0.53	0.23	0.13	0.11	0.02
$k_\parallel$ (σ_z=1mm)	[V/pC]	1.36	1.71	1.46	1.25	1.27	0.85

Evolution of inner cells proposed for the ILC collider

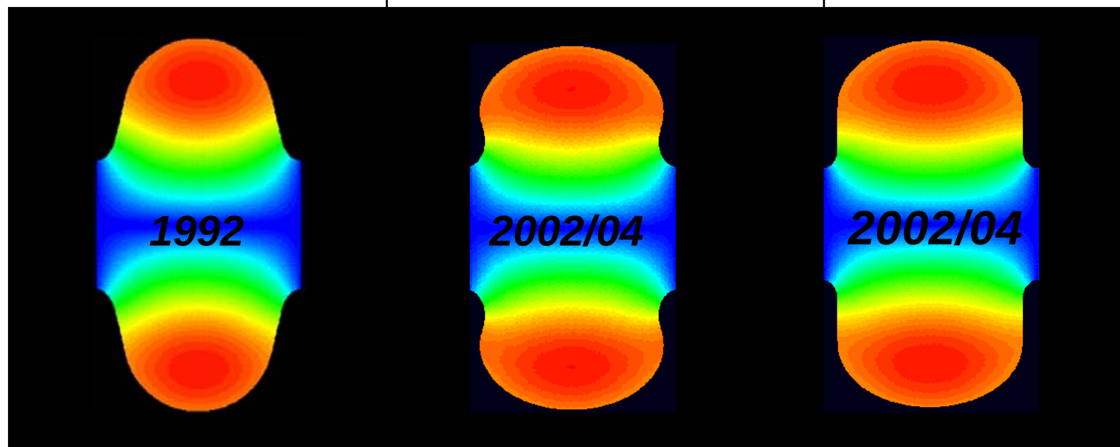

		TESLA optimized E_{peak}/E_{acc}	Re-entrant optimized B_{peak}/E_{acc}	LL optimized B_{peak}/E_{acc}
r_i	[mm]	35	30	30
k_{cc}	[%]	1.9	1.56	1.52
E_{peak}/E_{acc}	-	1.98	2.30	2.36
B_{peak}/E_{acc}	[mT/(MV/m)]	4.15	3.57	3.61
R/Q	[Ω]	113.8	135	133.7
G	[Ω]	271	284.3	284
R/Q*G	[Ω*Ω]	30840	38380	37970
$k_\perp$ (σ_z=1mm)	[V/pC/cm²]	0.23	0.38	0.38
$k_\parallel$ (σ_z=1mm)	[V/pC]	1.46	1.75	1.72

Multipacting

It is a phenomenon of resonant electron emission and multiplication.

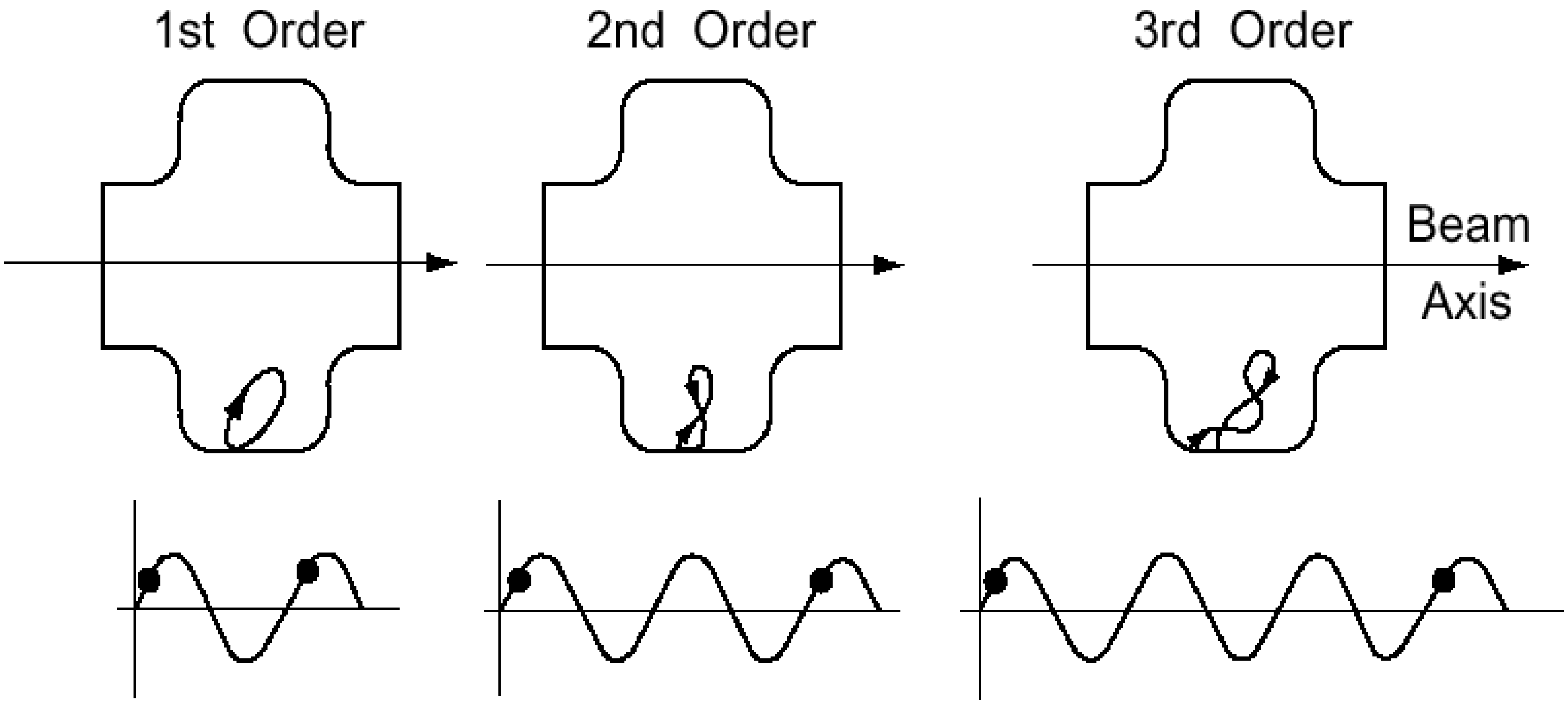

Curtsey W. Hartung

Impacting electron might create more than one secondary electron. This depends on the impact energy *K* and secondary emission yield *δ(K)* .

SEY is function of the impact energy *K* and depends on the surface cleanness.

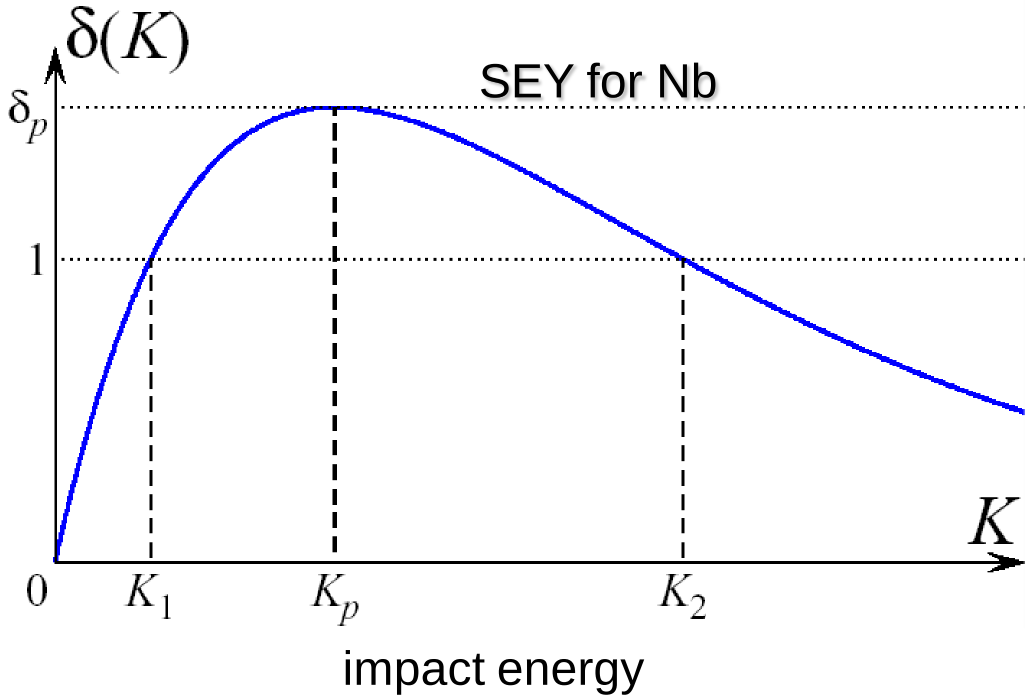

Condition	K_1	K_2
high SEY	~ 27 eV	$\gtrsim 2000$ eV
typical SEY	~ 40 eV	~ 1000 eV
low SEY	~ 150 eV	~ 750 eV

When happens, multipacting is barrier in rising the accelerating field in cavities and usually leads to quench.

In the design process we need to prove whether or not the shape of cell allows for multipacting.

LL; KEK test September 2005

f	[MHz]	1286.6
E_{peak}/E_{acc}	-	1.86
B_{peak}/E_{acc}	[mT/(MV/m)]	3.71
R/Q	[Ω]	130.0
G	[Ω]	279
$Ø_{iris}$	[mm]	61

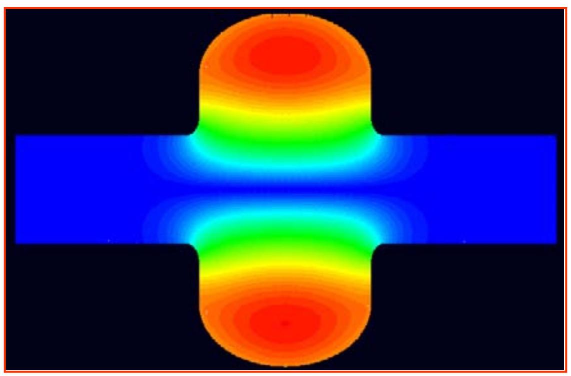

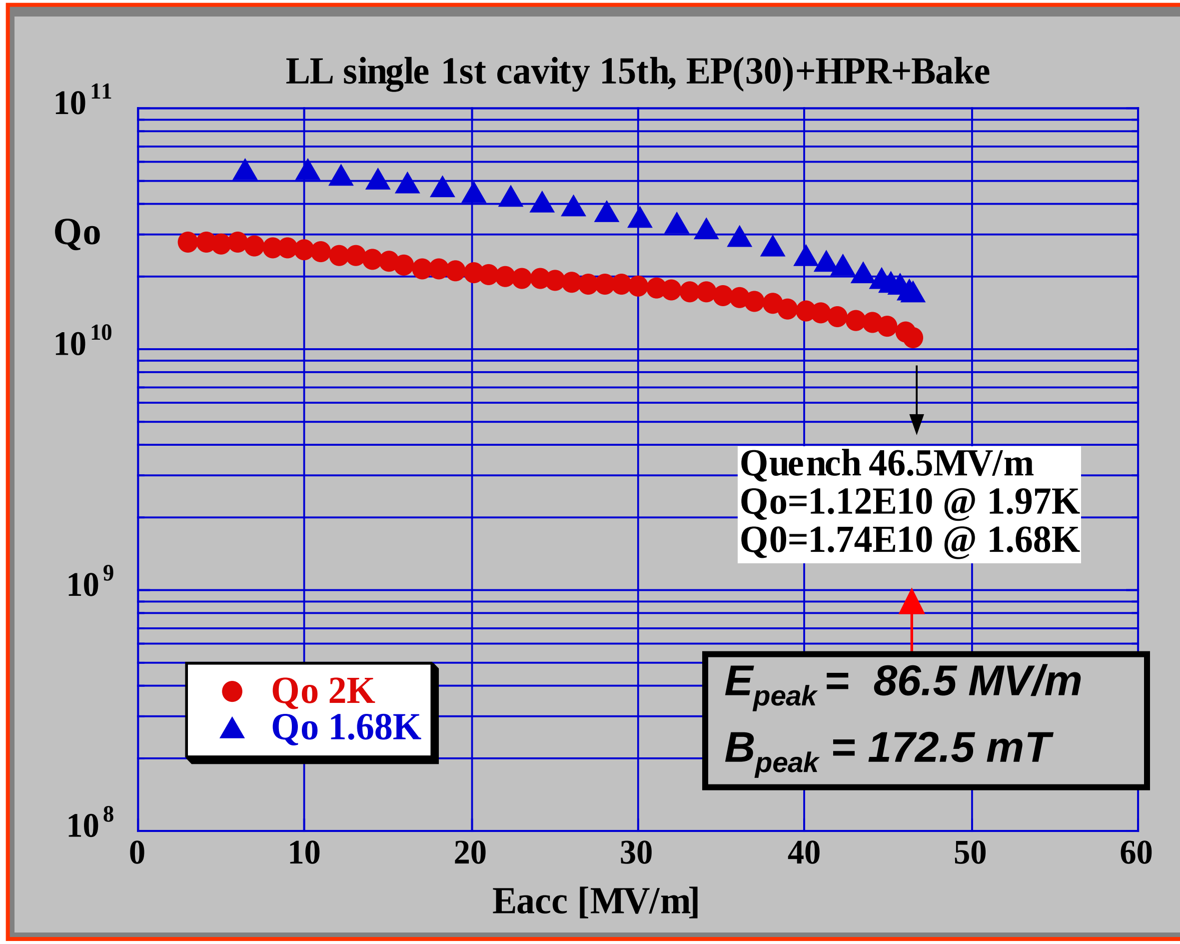

RE; Cornell, test in March 2007 !!!!

f	[MHz]	1300.3
E_{peak}/E_{acc}	-	2.11
B_{peak}/E_{acc}	[mT/(MV/m)]	3.53
R/Q	[Ω]	126.0
G	[Ω]	283.3
$Ø_{iris}$	[mm]	60

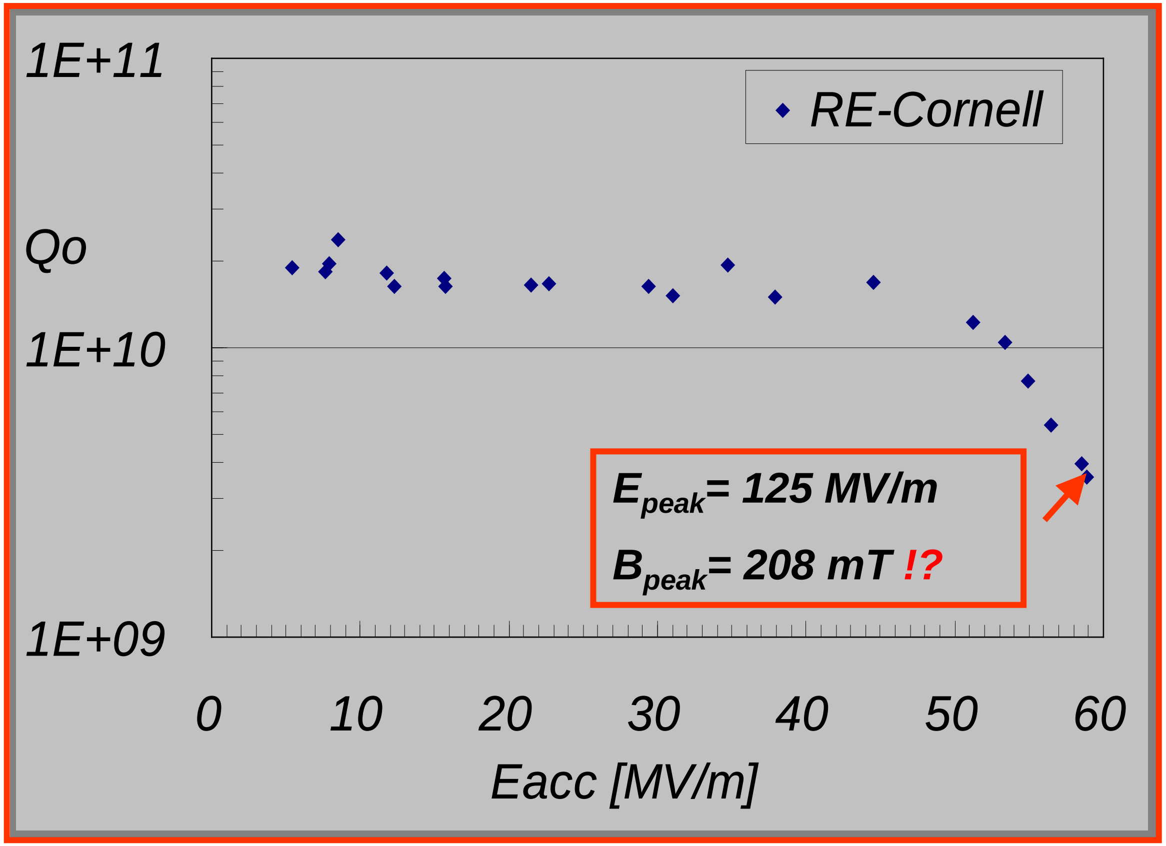

We re-call pros and cons for a multi-cell structure:

- Cost of accelerators is lower (less auxiliaries: LHe vessels, tuners, fundamental power couplers, control electronics……..)
- Higher real-estate gradient (better fill factor)
- Field flatness vs. N
- HOM excitation and trapping vs. N
- Power capability of fundamental power couplers vs. N
- Surface cleaning procedures become more complicated
- The worst performing cell limits whole multi-cell structure

Accelerating mode in multi-cell structures

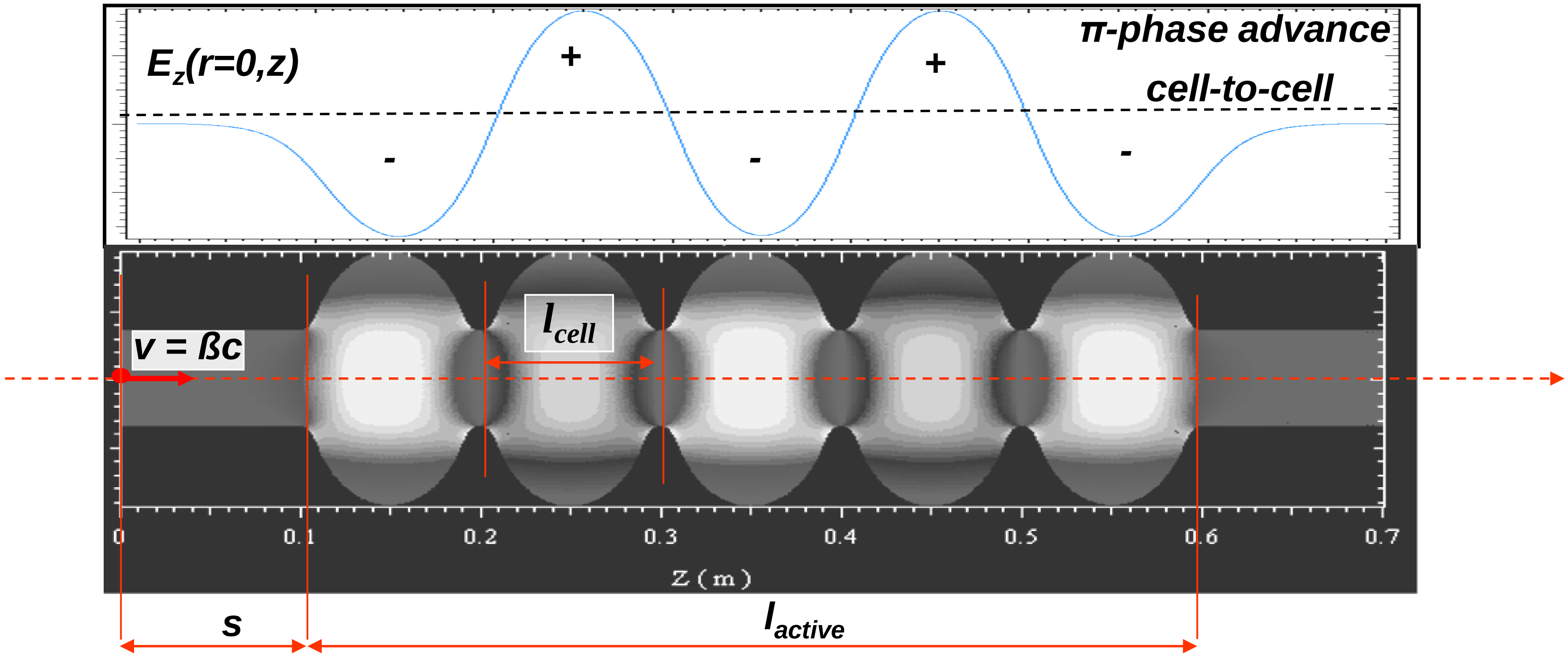

Synchronic acceleration and max of $(R/Q)_{acc}$ for a multi-cell structure when:

1. $l_{active} = Nl_{cell} = Nc\beta/(2f)$ and

2. the injection takes place at an optimum phase φ_{opt}, which ensures that particles arrive at the mid-plane of the first cell when E_{acc} reaches its maximum (minimum)

Field flatness in multi-cell structures

	Original Cornell N = 5	High Gradient N =7	Low Loss N =7	TESLA N=9	SNS ß=0.61 N=6	SNS ß=0.81 N=6	Low Loss N =9	RHIC N=5
year	1982	2001	2002	1992	2000	2000	2003	2003
a_{ff}	1489	2592	3288	4091	3883	2924	5435	850

$$a_{ff} = \frac{N^2}{k_{cc} \cdot ß}$$

Decades of experience with: heat and chemical treatment, handling and assembly allow to maintain good field profile, even in cavities with bigger N and weaker k_{cc}.

For many TESLA cavities: field flatness is better than 95 %

HOM excitation and trapping in multi-cell structures

HOM excitation causes:

- Beam instabilities and/or dilution of emittance
- Bunch-to-bunch energy modulation
- Additional cryogenic loss

HOM excitation:

Time structure of the beam

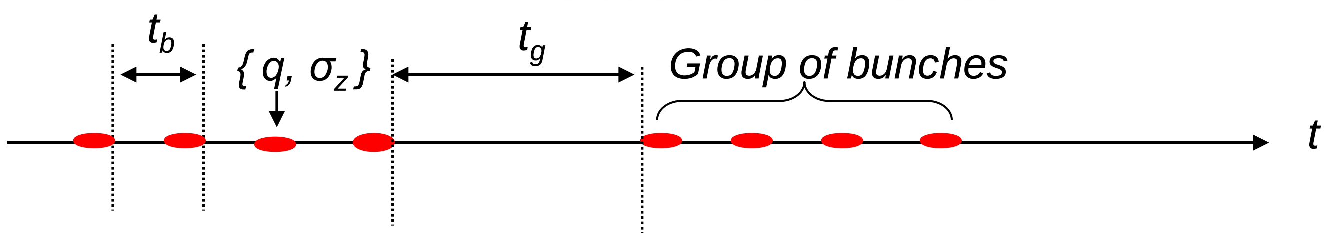

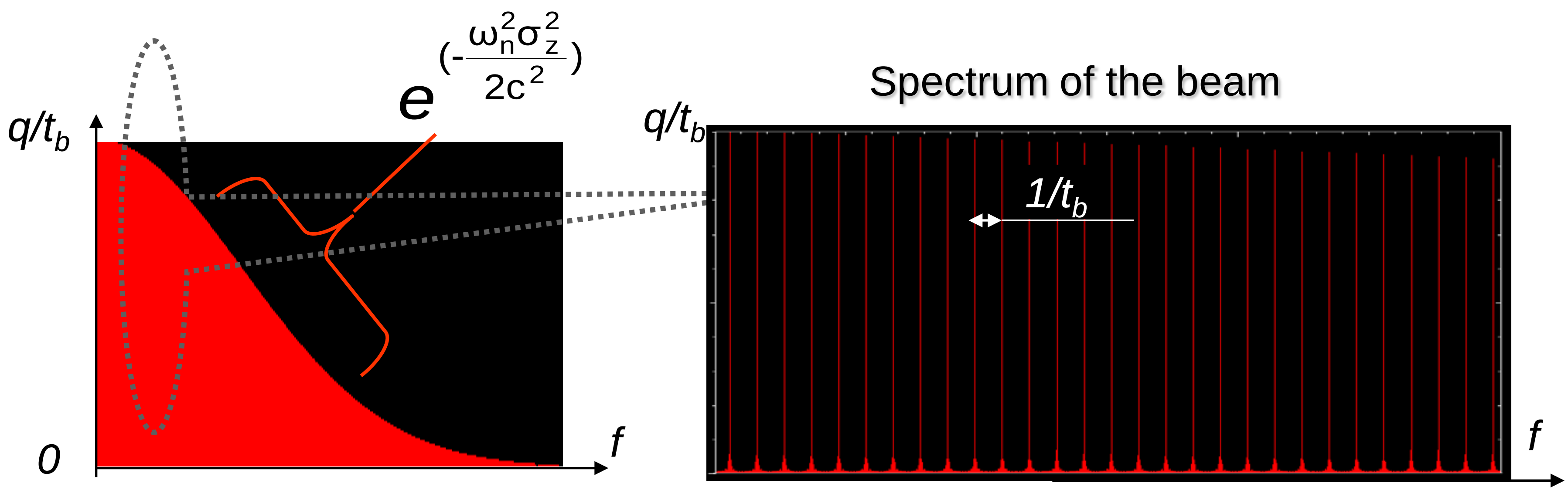

Mode No. n : $\{ \omega_n, (R/Q)_n, Q_{L,n} \}$

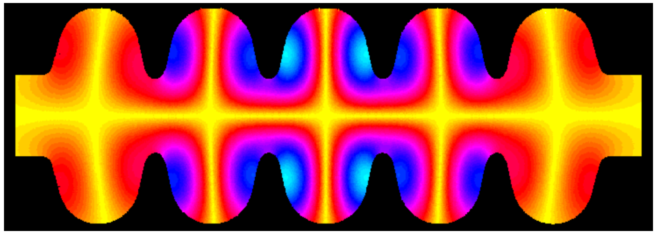

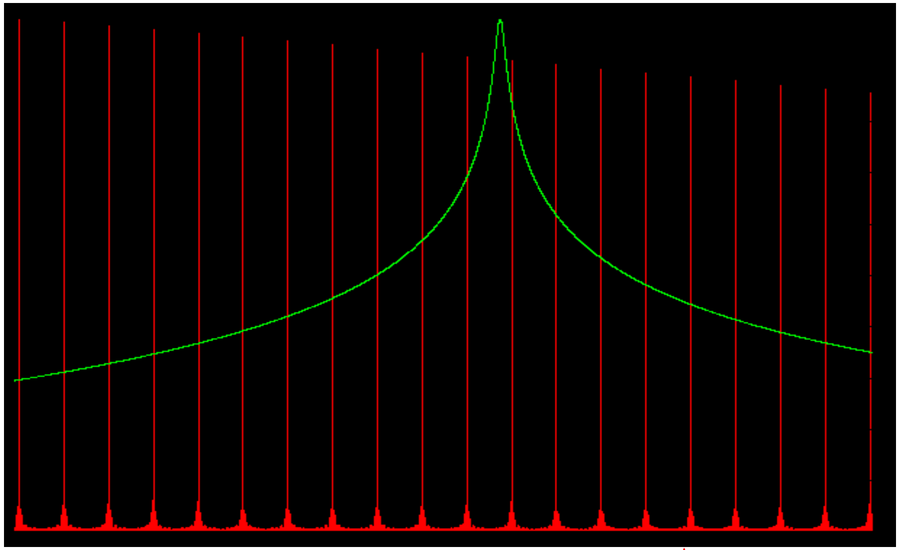

$$\underbrace{Z_n(\omega) = \frac{(R/Q)_n \cdot Q_{L,n}}{1 + jQ_{L,n}\left(\frac{\omega}{\omega_n} - \frac{\omega_n}{\omega}\right)}}$$

Impedance of the n-mode

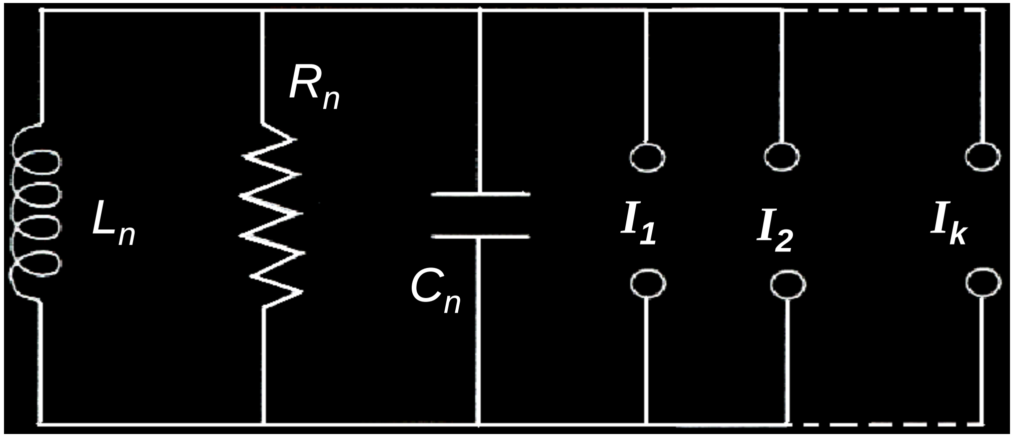

Multi-source excitation

The power induced by “all” spectral lines (current sources) in mode No. *n*:

$$P_n = \frac{1}{2}\sum_k Z_n(\omega_k)\cdot I_k^2$$

$$Z_n(\omega) = \frac{(R/Q)_n \cdot Q_{L,n}}{1 + jQ_{L,n}\left(\frac{\omega}{\omega_n} - \frac{\omega_n}{\omega}\right)}$$

where:

$$\frac{1}{Q_{L,n}} = \frac{1}{Q_{0,n}} + \frac{1}{Q_{ext,n}}$$

Measure of the extracted power

The HOM couplers, devices extracting the energy from parasitic modes, are attached to cavities for mitigation of high and harmful *E-M* fields of HOM .

The experience is that, the HOM couplers can be attached to the beam tubes and must not be located at cells because this leads to the performance degradation.

Coaxial HOM coupler

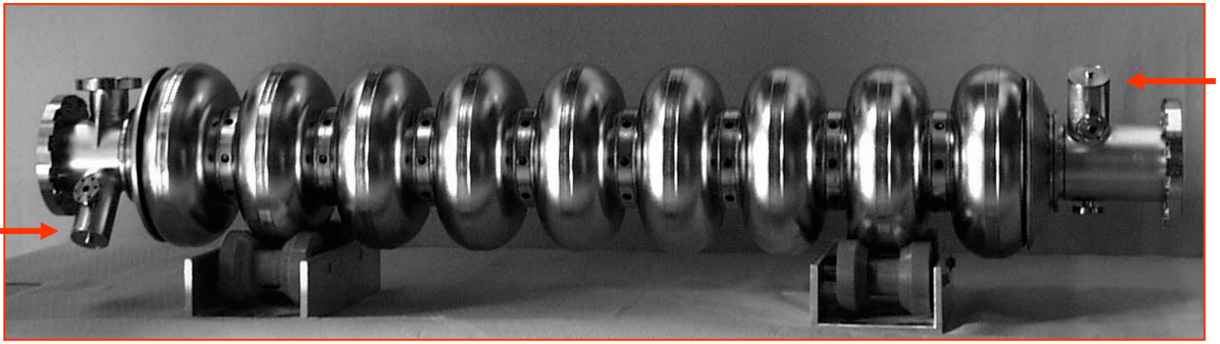

Coaxial HOM coupler

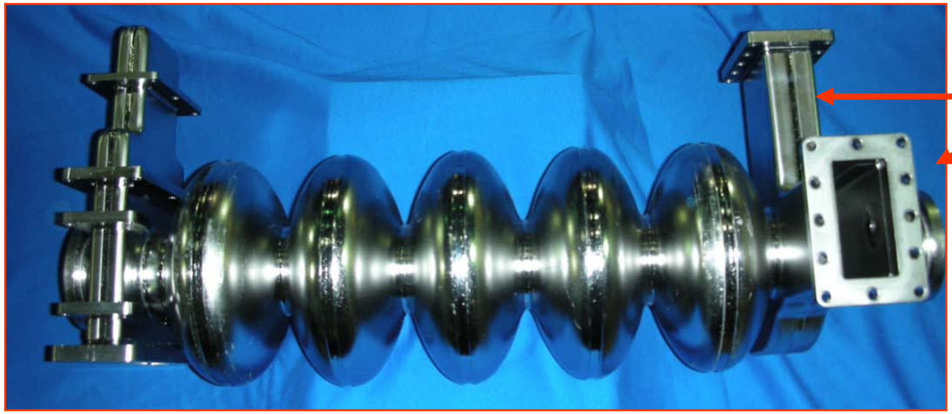

Waveguide HOM ports

The HOM trapping is similar to the FM field profile unflatness mechanism:

- weak $k_{cc,HOM}$, cell-to-cell coupling for HOM
- difference in the HOM frequency between the end-cells and inner-cells

f = 2385 MHz

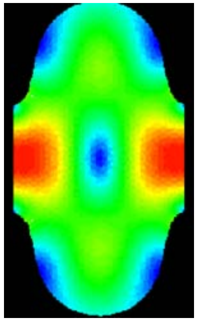

That is why they hardly resonate together

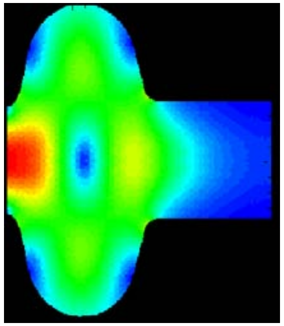

f = 2415 MHz

Example of the trapping and how *N* influences strength of the *E-H* fields at the HOM couplers locations

no *E-H* fields at HOM couplers locations (<u>trapping</u>), which are always placed at the end beam tubes

N = 17

N = 13

N = 9

N = 5

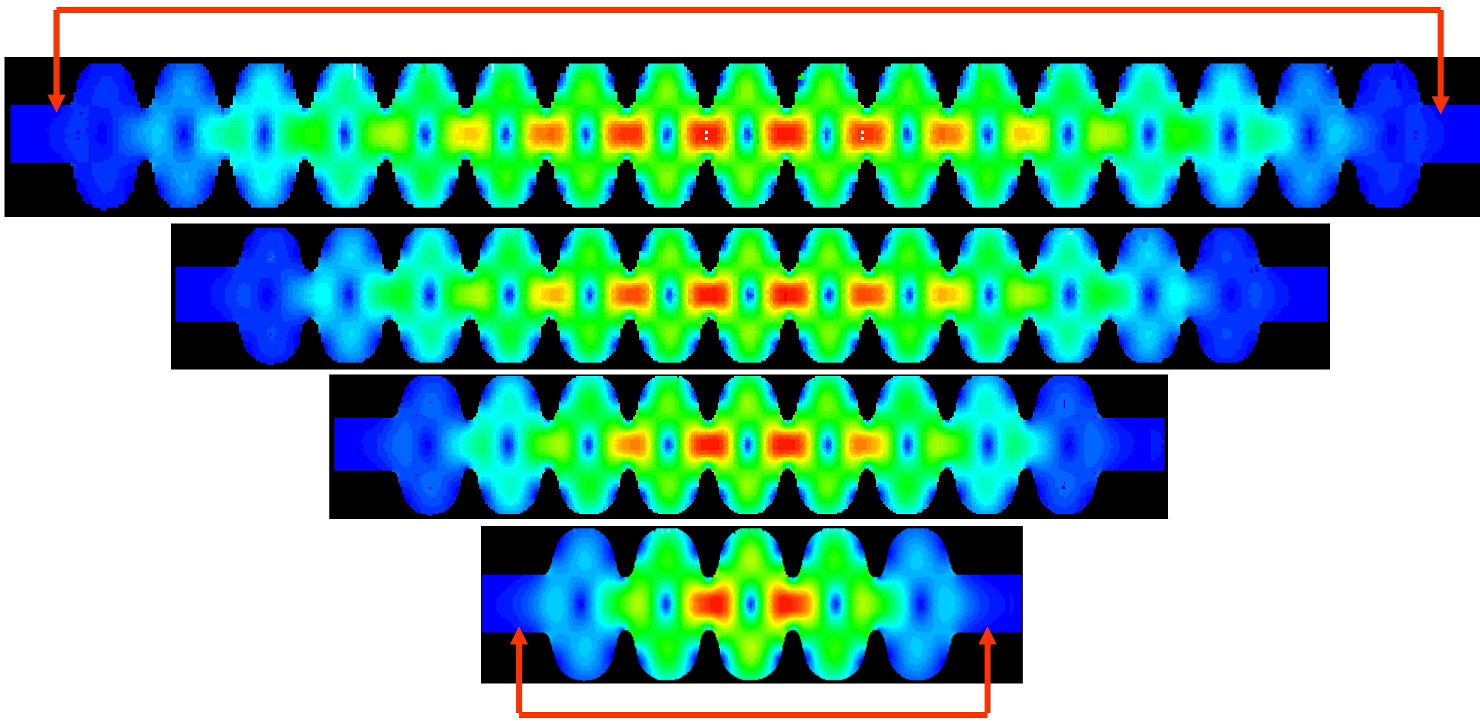

E-H fields at HOM couplers locations

Less cells in a structure helps always to reach low Qs of HOMs.

What else can help to avoid the trapping?

Adjustment of end-cells

The geometry of end-cells differs from the geometry of inner cells due to the attached beam tubes, HOM- and input couplers.

Their function is multifold and their geometry must fulfill three requirements:

- field flatness and frequency of the accelerating mode
- field strength of the accelerating mode must enable matching of Qext of FPC
- field strength of the dangerous HOMs must ensure required damping.

All three requirements make design of the end-cells more difficult than inner cells.

1. Open irises of the inner- and end-cells (bigger $k_{cc,HOM}$) and shaping them similarly.

Example: RHIC 5

Monopole mode k_{cc}

f_{HOM} = 1394 MHz

f_{HOM} = 1403 MHz

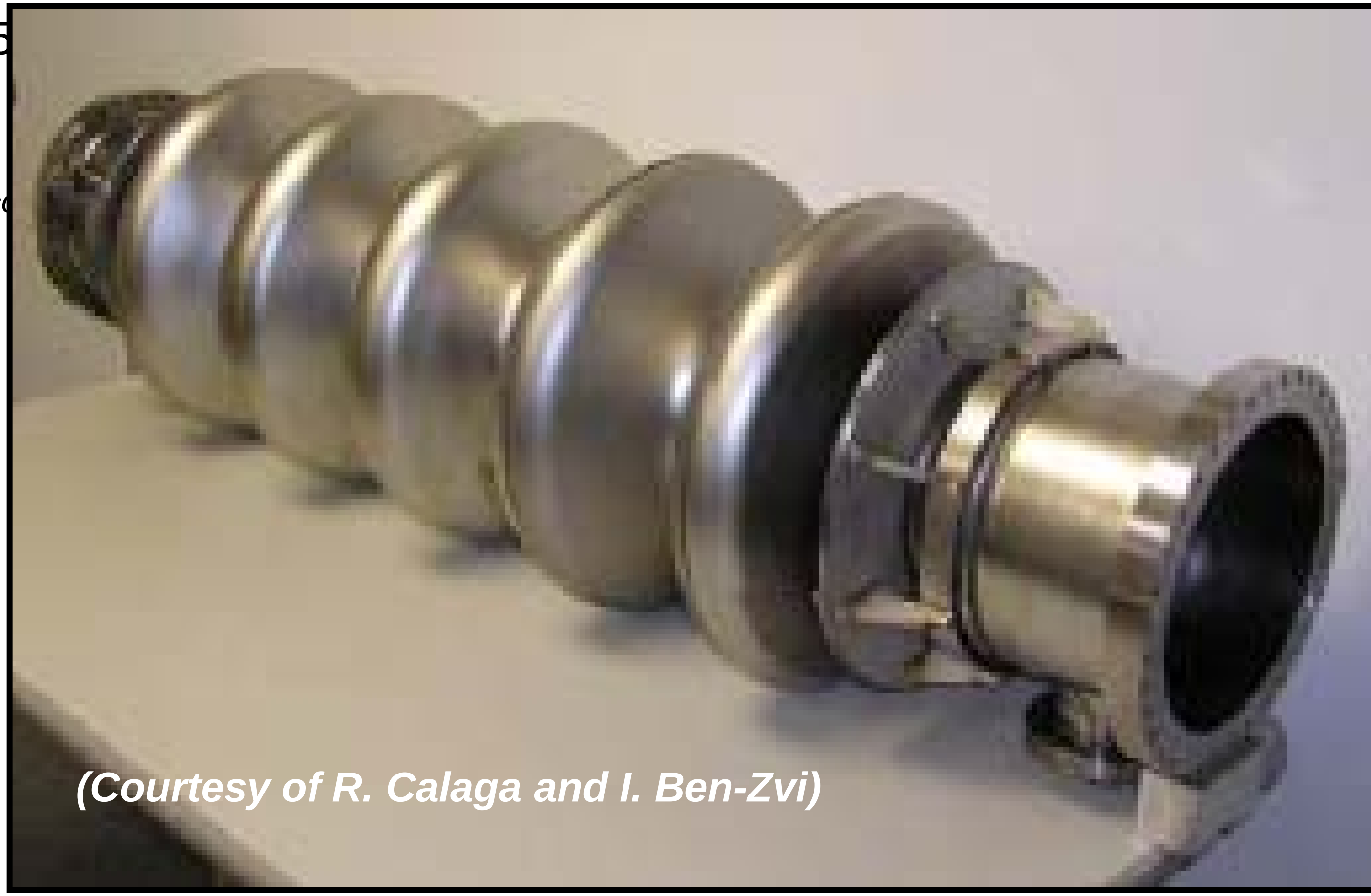

(Courtesy of R. Calaga and I. Ben-Zvi)

The method causes (R/Q) reduction of fundamental mode, which in this application is less relevant.

2. Tailoring the end-cells to equalize HOM frequencies of inner- and end-cells.

Example: TESLA 9-cell cavity, which has two different end-cells (asymmetric cavity)

The lowest mode in the passband f_{HOM} = 2382 MHz

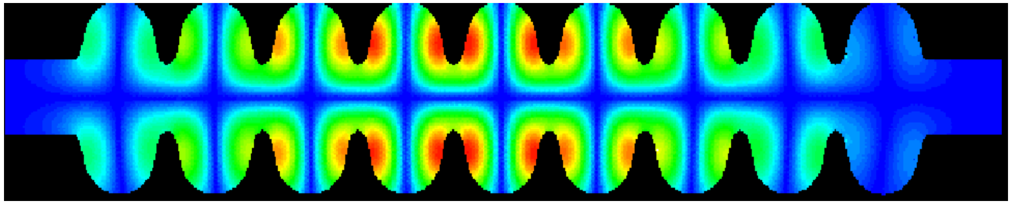

The highest mode in the passband f_{HOM} = 2458 MHz

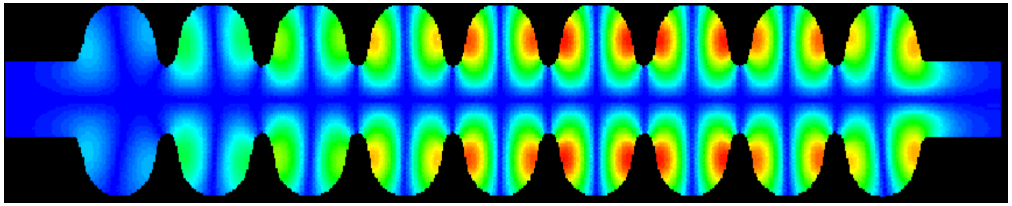

The method works for few modes but keeps the (R/Q) of the fundamental mode high.

5. Multi-cell Structures and Weakly Coupled Structures

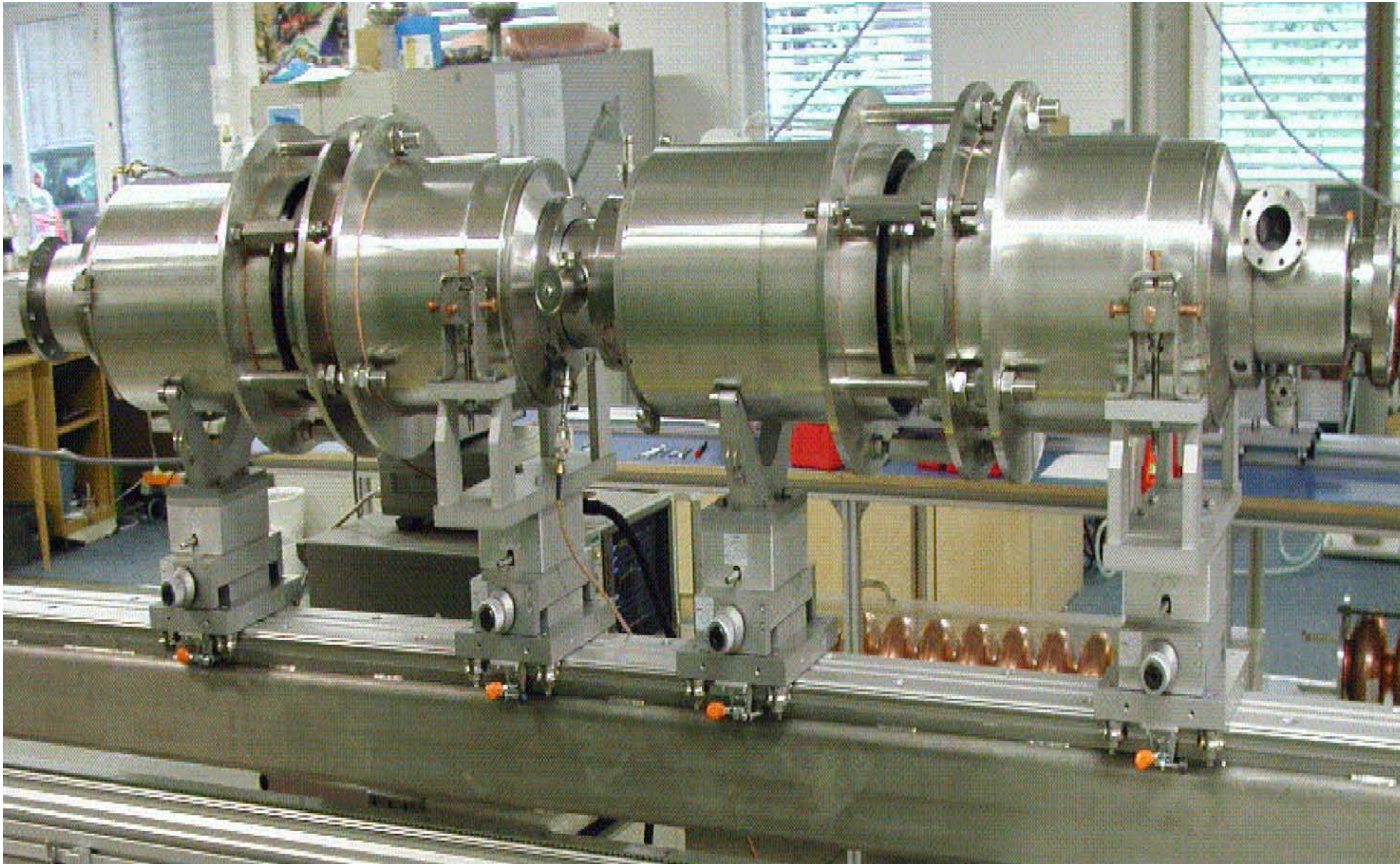

Power capability of the FPC for multi-cell structures

When I_{beam} and E_{acc} are specified and a superconducting multi-cell structure does not operate in the energy recovery mode:

$$P_{in} \sim N$$

Q_{ext} of the FPC, which usually is << than intrinsic Qo, is:

$$Q_{ext} \cong \frac{E_{acc} \cdot ß \cdot \lambda \cdot N}{I_{beam} \cdot (R/Q)_{cell} \cdot N} = \frac{E_{acc} \cdot ß \cdot \lambda}{I_{beam} \cdot (R/Q)_{cell}} = \frac{\omega_{acc} \cdot W_{onecell} \cdot N}{\frac{1}{2} \int_{S_{inputport}} E_{acc} \times H_{acc} ds}$$

Independent of N

It must be ~ N to keep the ratio constant

$$\int_{S_{inputport}} E_{acc} \times H_{acc} ds$$

Coupler must penetrate deeper in the beam tube or/and is placed closer to the end cell

Opening for the coupler must be bigger

Both perturb the cylindrical symmetry of the end tube and increase kick to the beam

The remedies are: alternating positions of couplers or double couplers

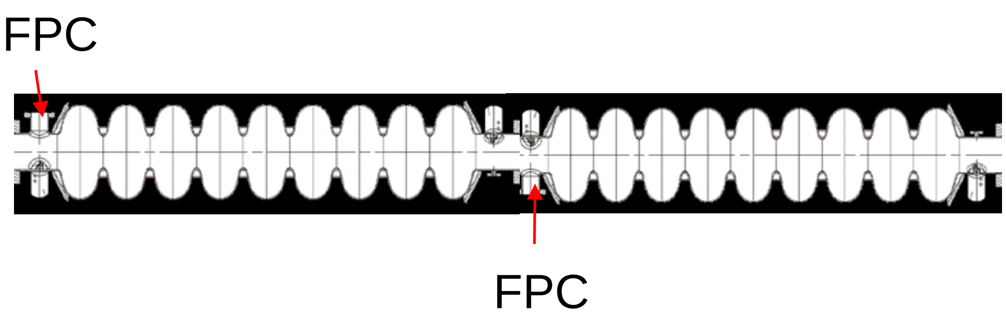

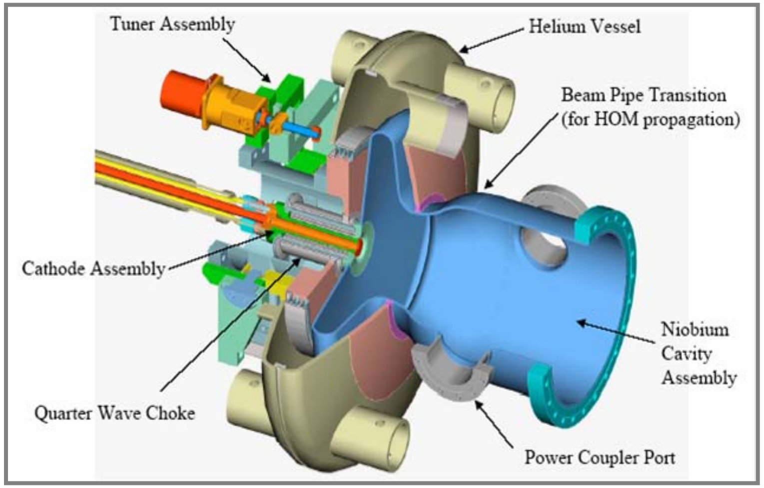

Courtesy of Alan Todd (AES)

Surface cleaning procedures are more complicated

Few words on Nb and on the surface preparation procedures

All high gradient cavities are made of the pure metallic bulk Nb (II-type sc, *Tc* = 9.2 K):

- We use poly-crystal Nb from the very beginning.
- Recently, we made several cavities of large-grain Nb (with hope for single crystal)

Surface preparation has several steps with three major procedures:

- Chemical treatment: can be Buffered Chemical Polishing or Electro-Polishing
- Heat treatment
- High Pressure Water rinsing

Buffered Chemical Polishing (BCP)

Acids: HF (49%), HNO_3 (65%), H_3PO_4 (85%)

Mixture: 1:1:1 or 1:1:2 by volume

Electro-Polishing (EP)

Electrolyte:

1 part HF(49%), 9 parts H_2SO_4 (96%)

Al-cathode, Nb-anode, J~ 50 mA/cm²

The sequence in the surface preparation is:

- Heavy chemical etch (EP or BCP)
  - Removal of damaged surface layer (100-150um) caused by fabrication and handling
- Removal of surface contamination
  - Ultrasonic cleaning of surface with detergent and DI water, or Alcohol rinse
- Heat treatment (600-800C in vacuum furnace)
  - Removes hydrogen from the bulk niobium to reduce the risk of Q-disease
- RF tuning and mechanical inspection
  - Field profile, calibration of test probes, check mechanical structure
- Removal of surface contamination
  - Ultrasonic cleaning of surface with detergent and DI water,
- Light chemical etch (EP or BCP)
  - Remove any risk from damage during handling and furnace contamination
- High pressure rinse (UPW @100 Bar) + Class 10 drying of cavity
  - Reduction of field emission sources, surface particulates
  - At least two passes over entire surface

Courtesy J. Mammosser

Example showing randomness in the performance due to the additional cleaning:
AC71 went from good to bad
AC76 went from bad to good

9-cell TESLA cavities

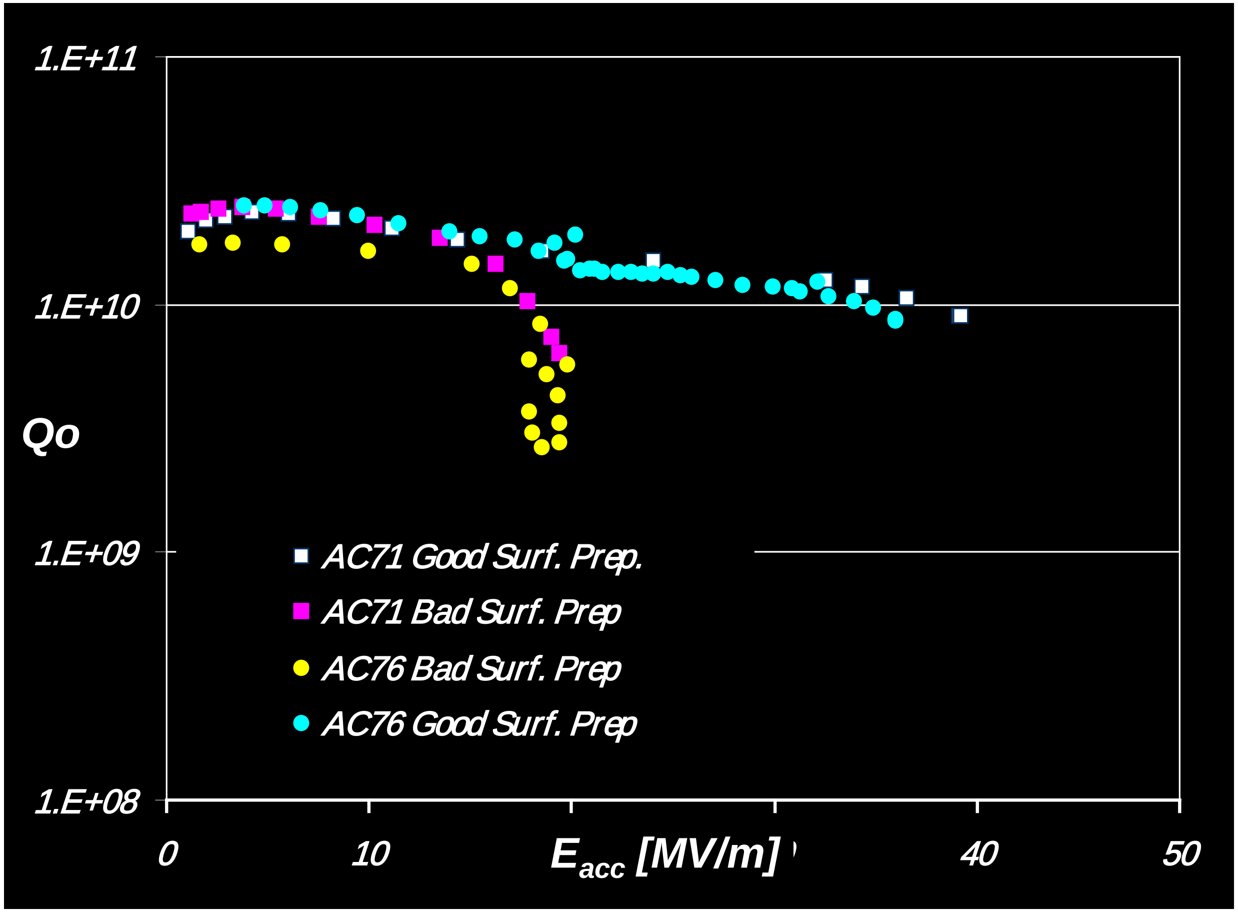

The best performance is still difficult to reach. The preparation must be repeated to reach the ultimate goal of 34 MV/m @ 10^{10}. It makes cavities very "expensive".

The worst performing cell limits whole multi-cell structure

After the pre-tuning all cells have the same amplitude

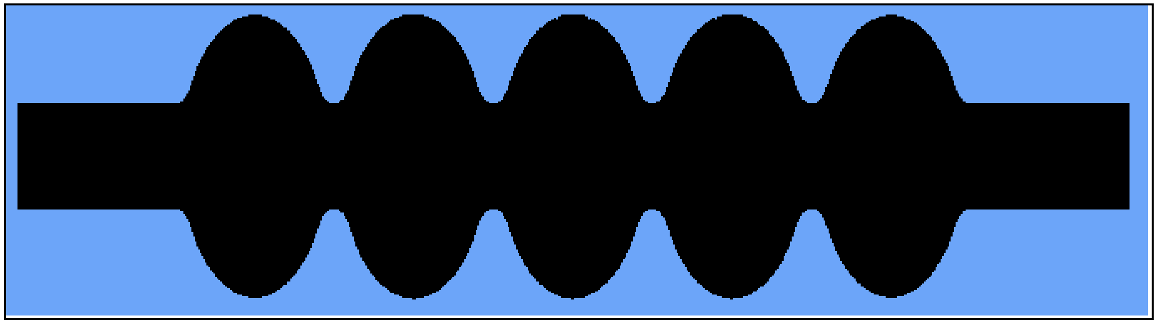

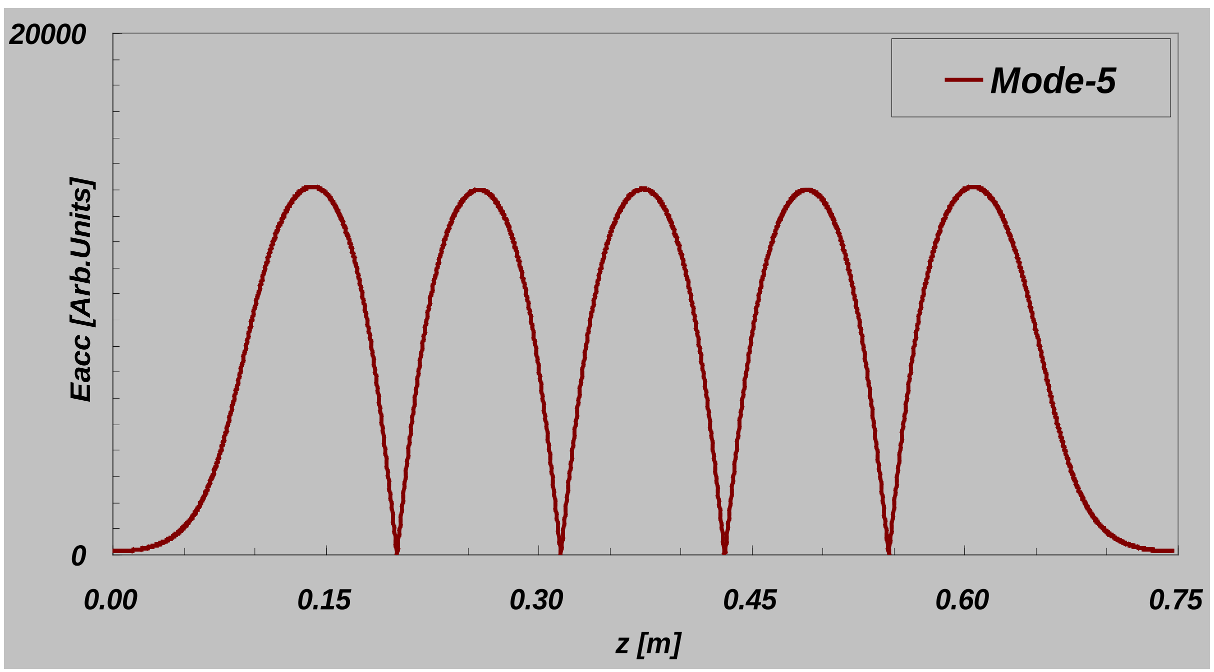

List of multi-cell cavities ß=1 optimized for various criteria

Criterion	Structure	Best parameter	Weakest parameter (point)	Comments
E_{acc}	*HG: 1.5 GHz, N=7* *TESLA: 1.3 GHz, N=9* *ILC-LL: 1.3 GHz, N=9* *ILC-RE 1.3 GHz, N=9*	*Epeak/Eacc= 1.96* *Epeak/Eacc= 1.98* *Bpeak/Eacc= 3.61* *Bpeak/Eacc= 3.57*	*maximum -Eacc* *maximum -Eacc* *Epeak/Eacc* *Epeak/Eacc*	*Designed for* I_{beam} *< 10 mA, Pulse operation*
P_{loss}	*LL: 1.5 GHz, N= 7*	*Bpeak/Eacc= 3.7* *(R/Q)·G*	*Not easy to clean, HOM damping*	*Designed for* I_{beam} *< 1 mA First LL-type cavity*
Z_{HOM}	*RHIC: 0.7 GHz, N= 5*	*Very low:* $k_\perp$, $k_\parallel$ *Epeak/Eacc= 1.98*	*Cryogenic losses*	*First cavity for* $I_{beam} \approx 2$ *A*

Design of an elliptical cavity is usually performed in two steps: “2D” and “3D” :

- “2D” is fast and allows to define geometry of a cylindrical symmetric body (inner and end-cells) of the cavity.
- “3D” is much more time consuming but necessary for modeling of full equipped cavity with FPC and HOM couplers.
  Also coupling strength for FPC and damping of HOMs can be modeled only in 3D.

Solutions to 2D (or 3D) Helmholtz equation can be found analytically only for very few geometries (pillbox, spherical resonators or rectangular resonator)

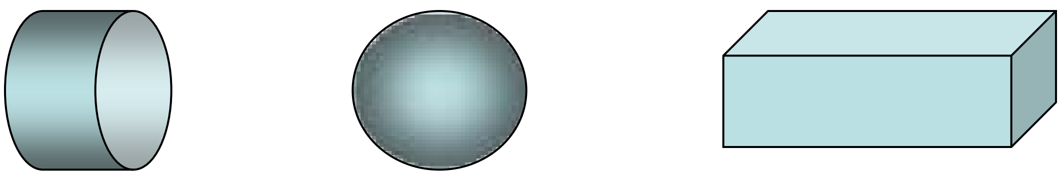

We need numerical methods: $$\underbrace{(\nabla^2 + \omega^2 \varepsilon\mu)}_{\text{Approximating operator}}\underbrace{A}_{\text{Approximating function}} = 0$$

Approximating operator
(Finite Difference Methods)

Approximating function
(Finite Element Methods)

The FEM is superior in mapping of curvilinear boundary. This is essential for modeling of:

- Multipacting
- Electron emission from the metal wall and generation of dark current
- Frequency change   )µm)

2D codes like SUPERFISH   ry
approx.) or FEM-code (3rd

Example from the FEM c   kage
MultiPac by P. Yla-Oijala ar

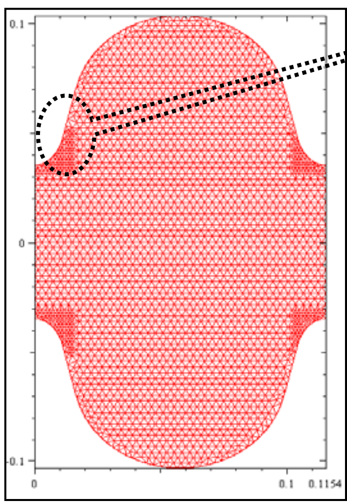

Smoo   the
force   by a
“zigza

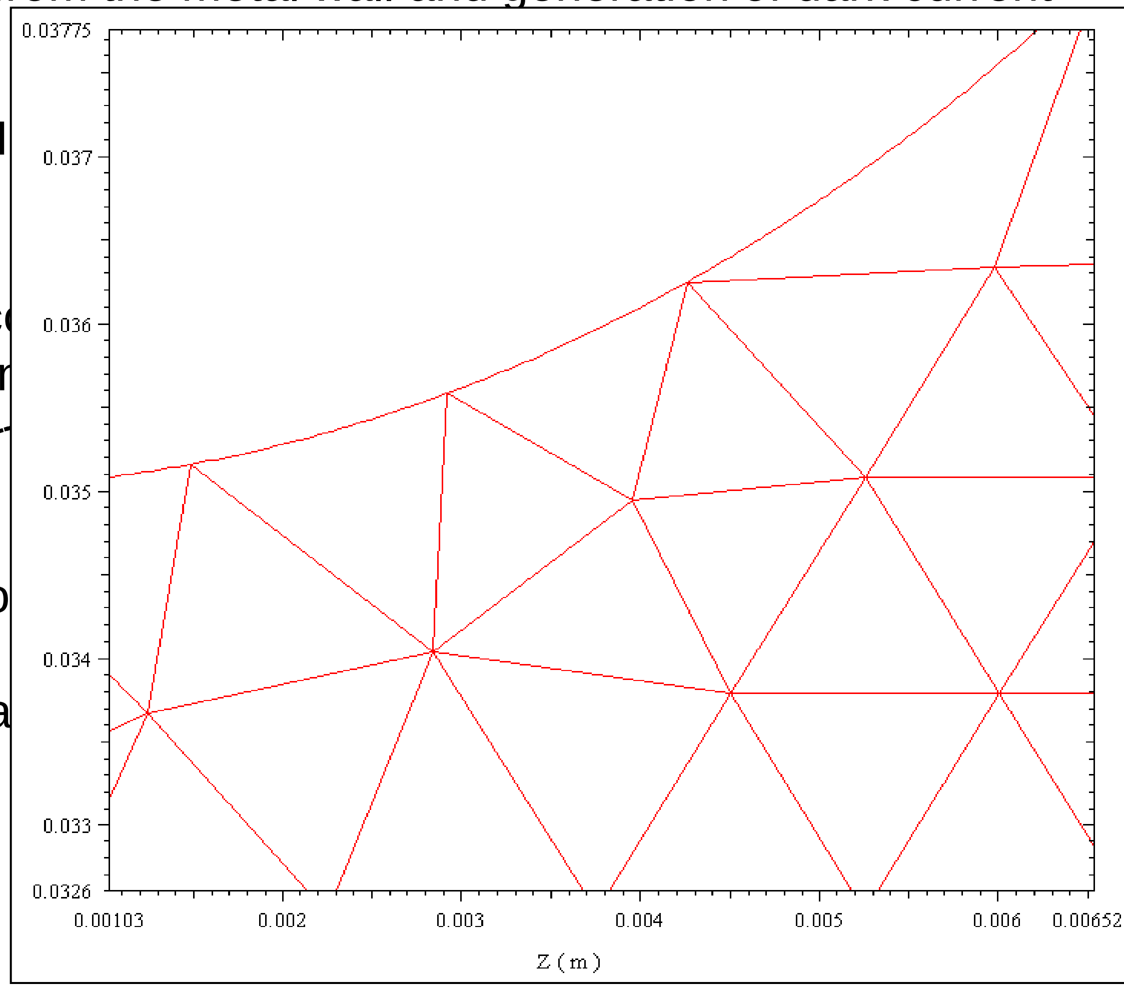

Example: FEM-code modeling of the frequency change due to the chemical treatment (removed layer of 100µm)

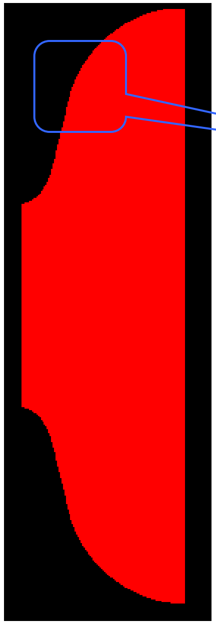

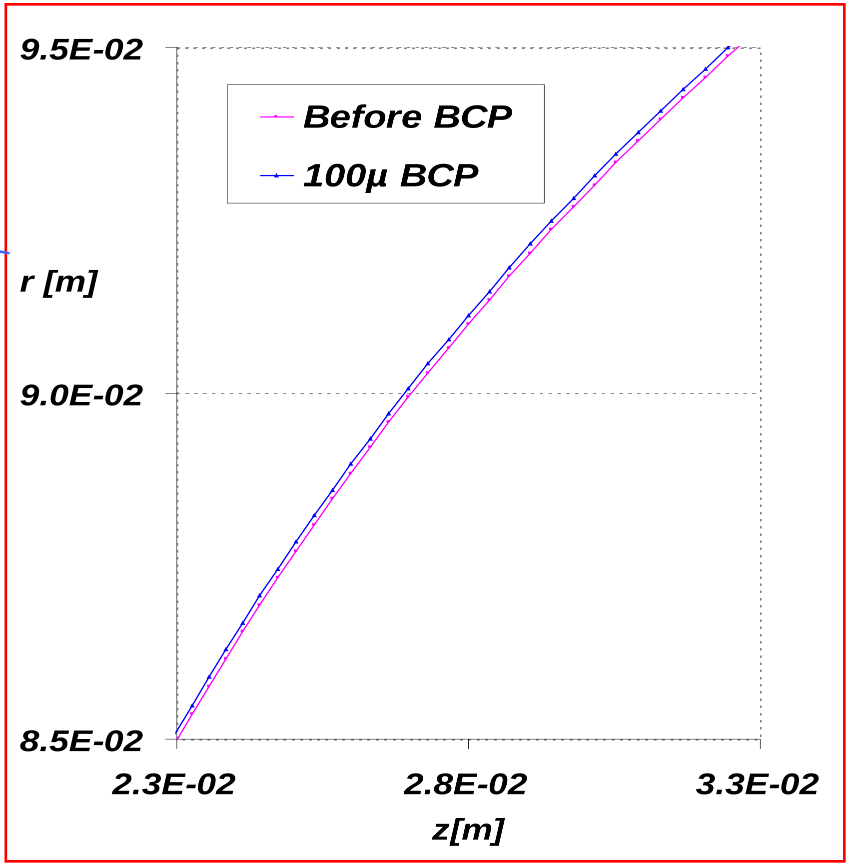

Zoomed difference in shape of the TESLA mid cup after 100µm BCP

2D Modeling takes ~2min

$$\frac{\partial f}{100\,\mu m} = -10kHz\,/\,\mu m$$

which was measured for the uniform removal

Electromagnetic Code Development at SLAC by ACD

Solves Maxwell's equations with particles in TD & FD

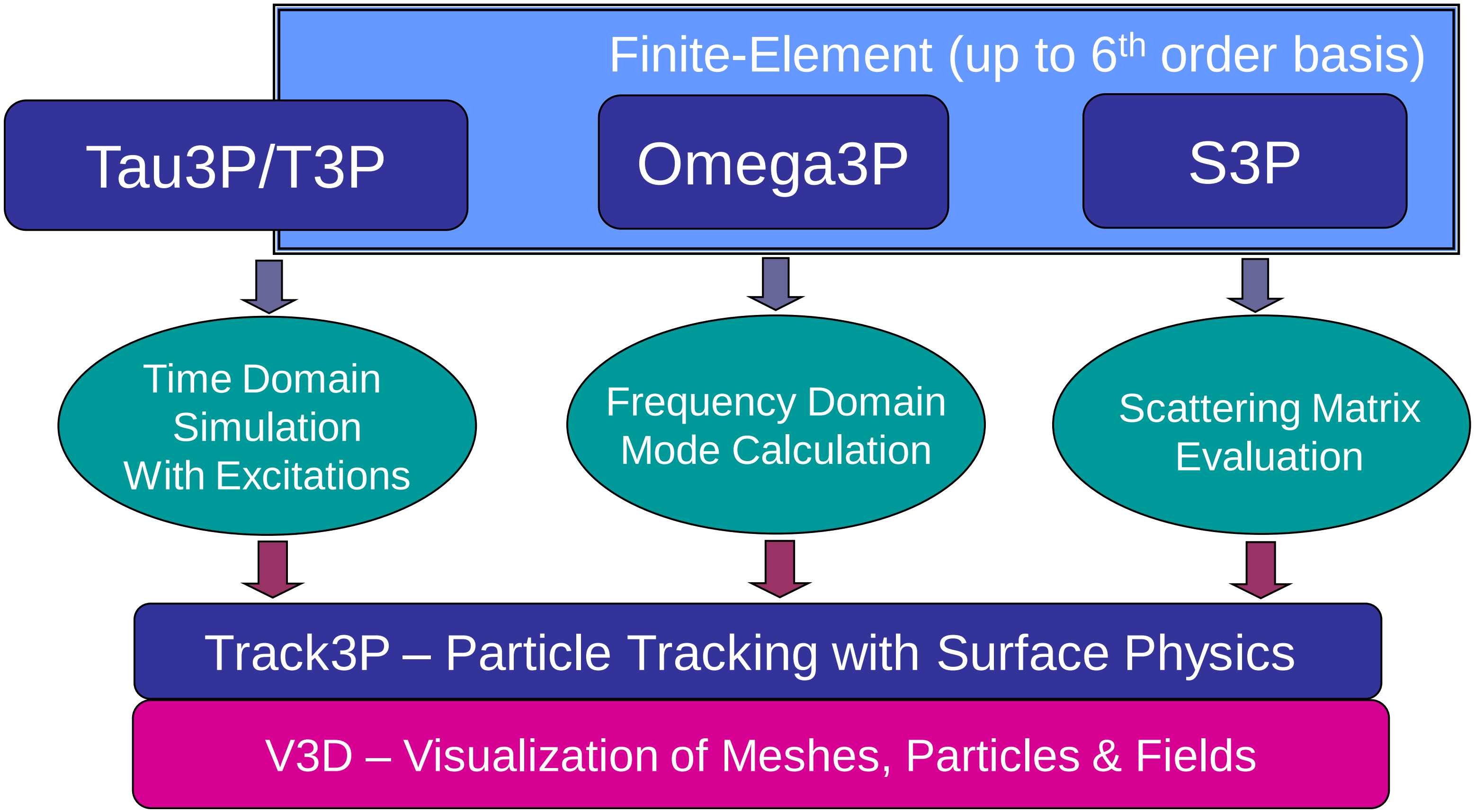

(Courtesy of Kwok Ko and ACD Members)

Example of 3D two dipoles overlapping modeling in the TESLA cavity with Omega3P

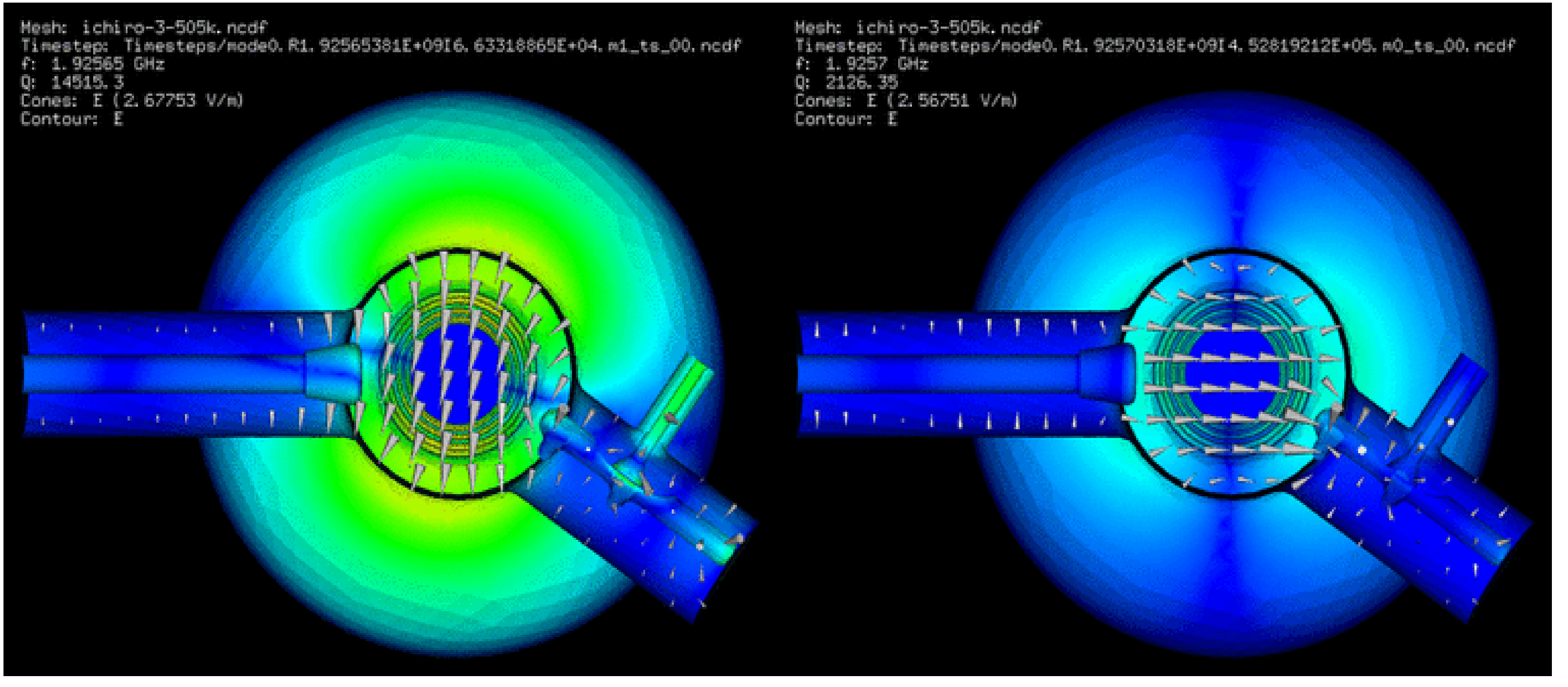

(Courtesy of Kwok Ko and ACD Members)

Example of 3D dipole damping modeling for the TESLA cavity with the coaxial coupling (Omega3P, L. Xiao, ACD SLAC)

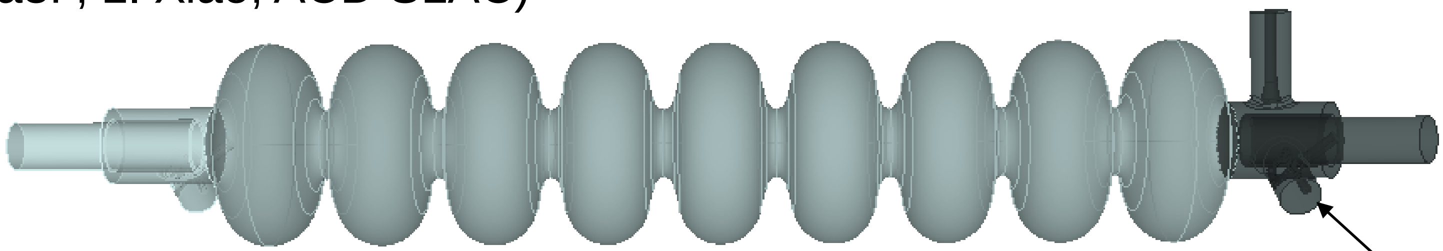

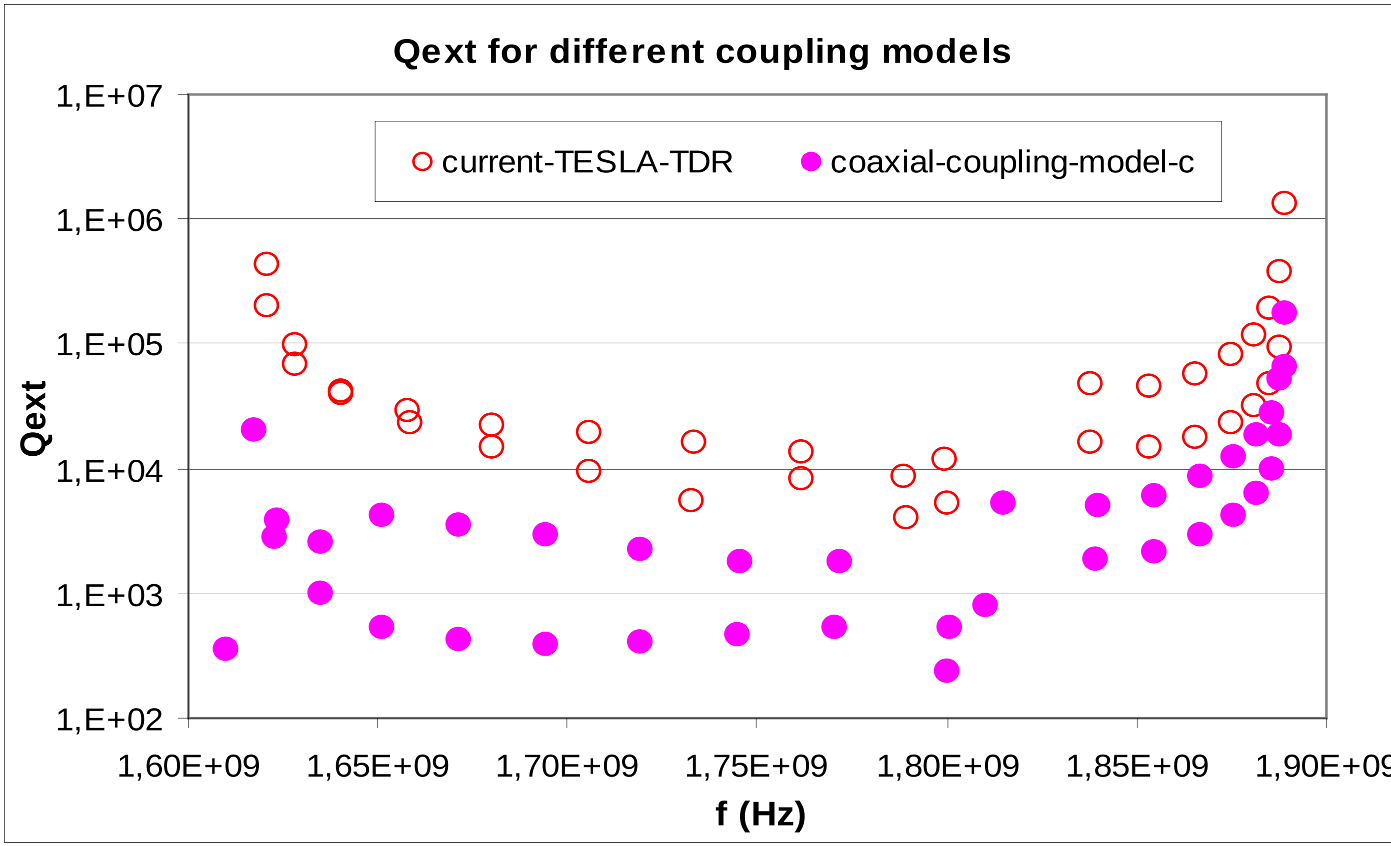

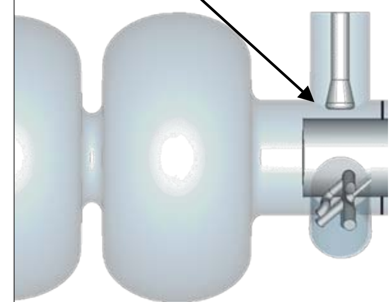

In the design process we use 2D-codes (*SUPERFISH, SLANS, FEM..)* and 3D-codes (MWS, HFSS, MAFIA and OMEGA-3P) but still the Lumped Element replacement Circuit is helpful to investigate some RF properties.

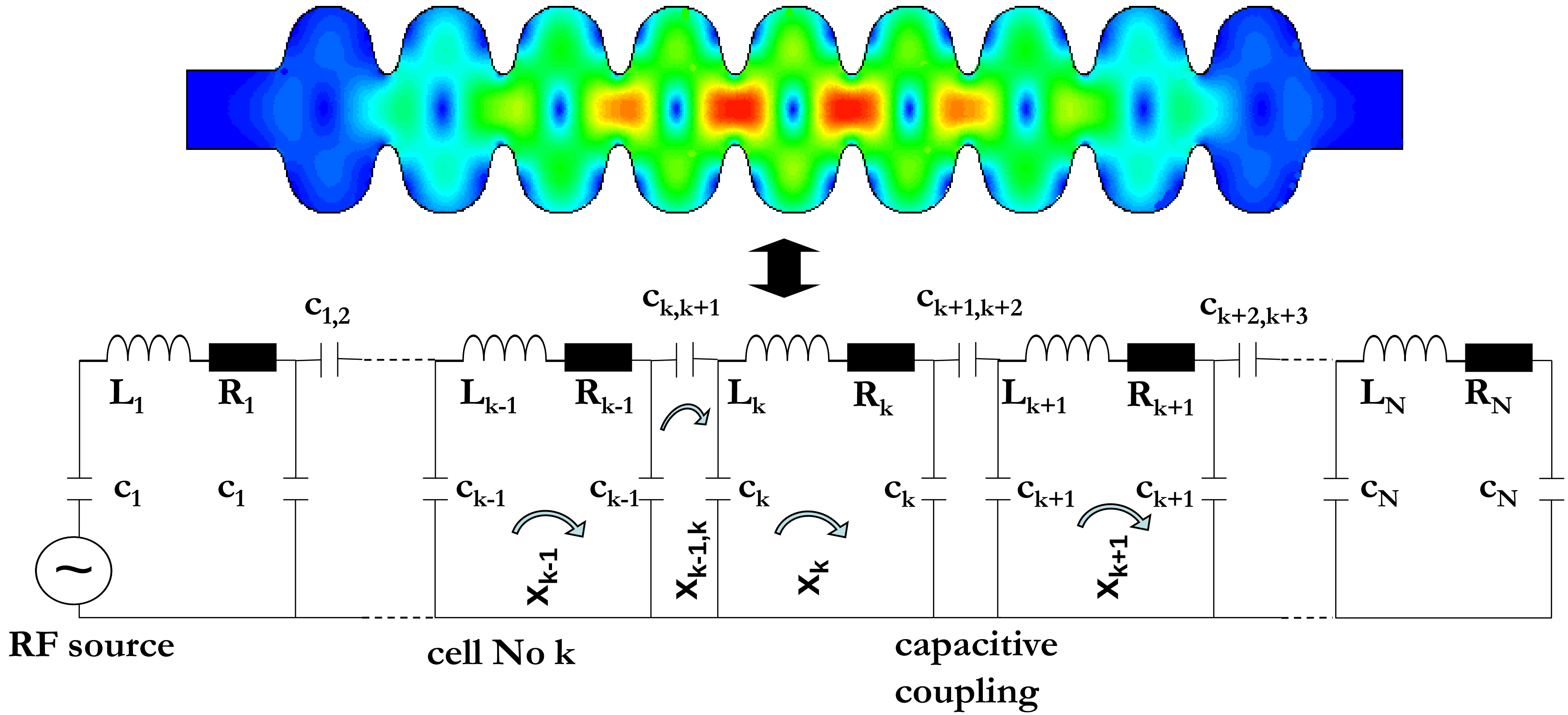

Where: $2\pi f_{FM} = (L_k \cdot c_k)^{-0.5}$; $(R/Q)_{FM} = (L_k/c_k)^{0.5}$; $R = (R/Q)_{FM} \cdot Q_{L,FM}$;

What can be done by means of the LEC:

- Cavity pre-tuning after the fabrication and bulk chemical treatment
- Investigation how the field profile in cells depends on their frequency errors ($\partial f/f<10^{-4}$)
- Investigation how passband frequencies depend on cell frequency errors ($\partial f/f<10^{-4}$)
- Modeling of the transient state (mode beating)
- Modeling of the voltage stability during acceleration

blue marked examples of the implementation are shown on next slides

Investigation of the FM passband frequencies sensitivity to cell frequency errors *($\partial f/f<10^{-4}$)*

Example: 7-cells, $k_{cc}=1.85\%$, 1st cell detuned by *-30kHz* (cell length changed -11µm !!, hard to model with 2D and 3D codes)

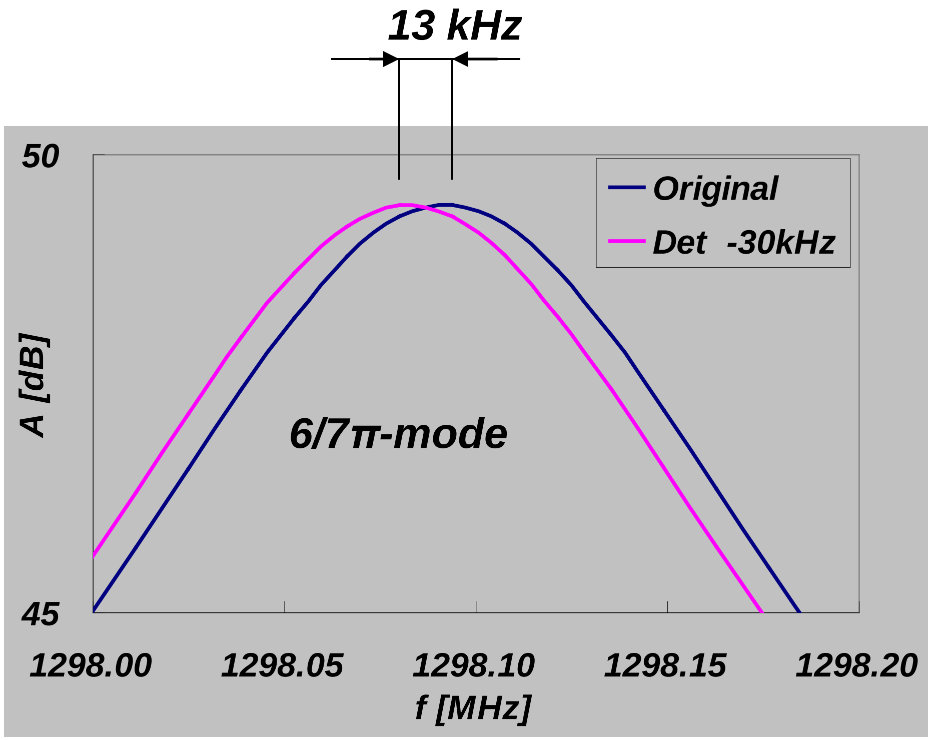

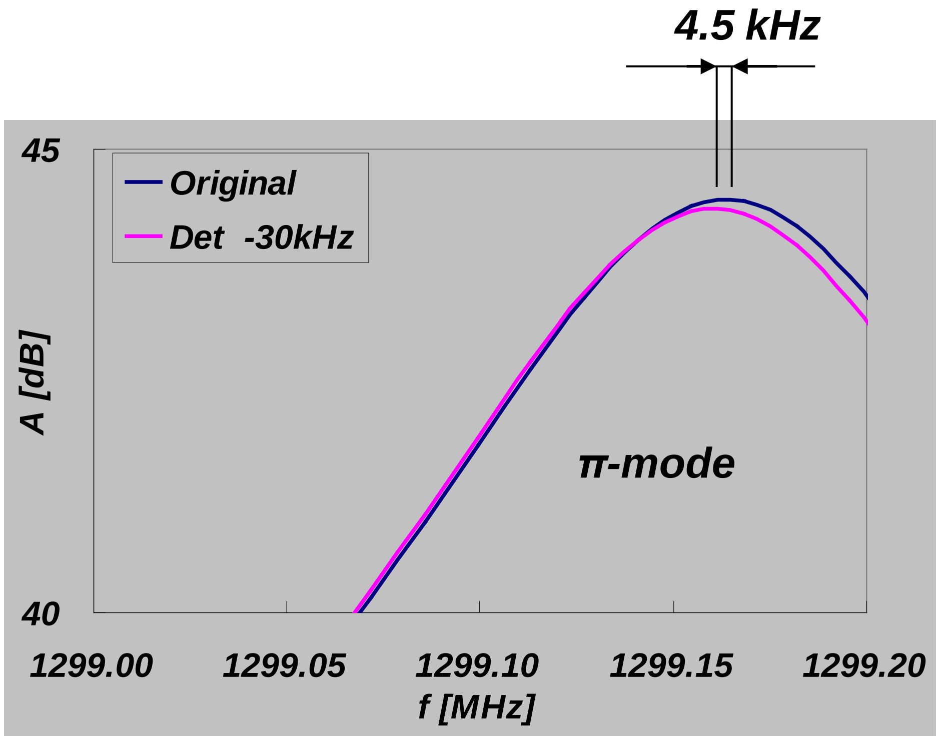

Transient State: Mode beating in the pulse operation

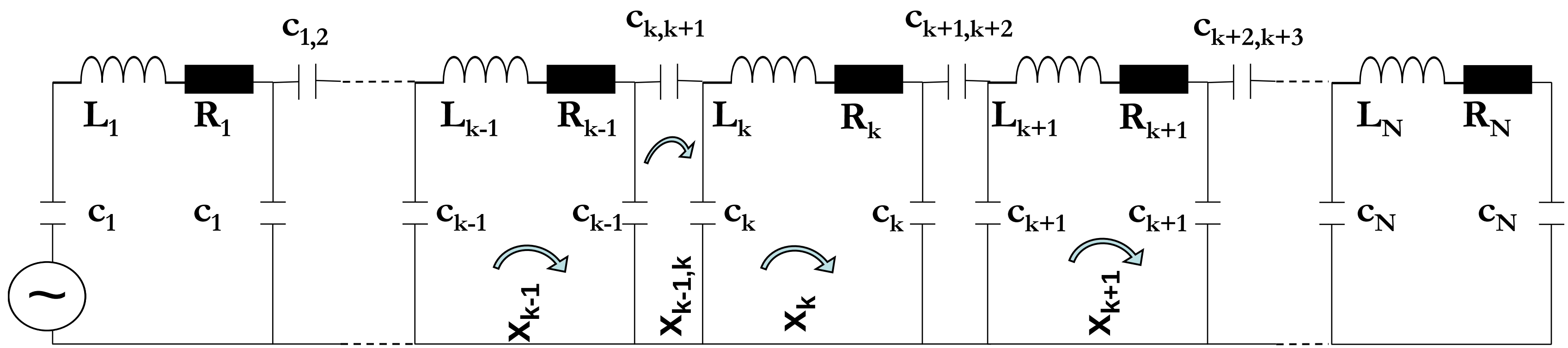

Solving the set of Kirchoff equations:

$$R_1 \cdot x_1(t) + L_1 \cdot \dot{x}_1(t) + \frac{1}{c_1} \cdot \int_0^t x_1(\tau)d\tau - \frac{1}{c_1} \cdot \int_0^t x_{1,2}(\tau)d\tau = U_{-1}(t) \cdot e(t)$$

....

$$-\frac{1}{c_k} \cdot \int_0^t x_{k-1,k}(\tau)d\tau + R_k \cdot x_k(t) + L_k \cdot \dot{x}_k(t) + \frac{1}{c_k} \cdot \int_0^t x_k(\tau)d\tau - \frac{1}{c_k} \cdot \int_0^t x_{k,k+1}(\tau)d\tau = 0$$

....

$$-\frac{1}{c_N} \cdot \int_0^t x_{N-1,N}(\tau)d\tau + R_N \cdot x_N(t) + L_N \cdot \dot{x}_N(t) + \frac{1}{c_N} \cdot \int_0^t x_N(\tau)d\tau = 0$$

one can find voltages right after the RF-source is switched on and during the acceleration

Modeling of the transient state (mode beating)

Example: 7-cells, k_{cc}=1.85%, Q_L=3.4 10^6

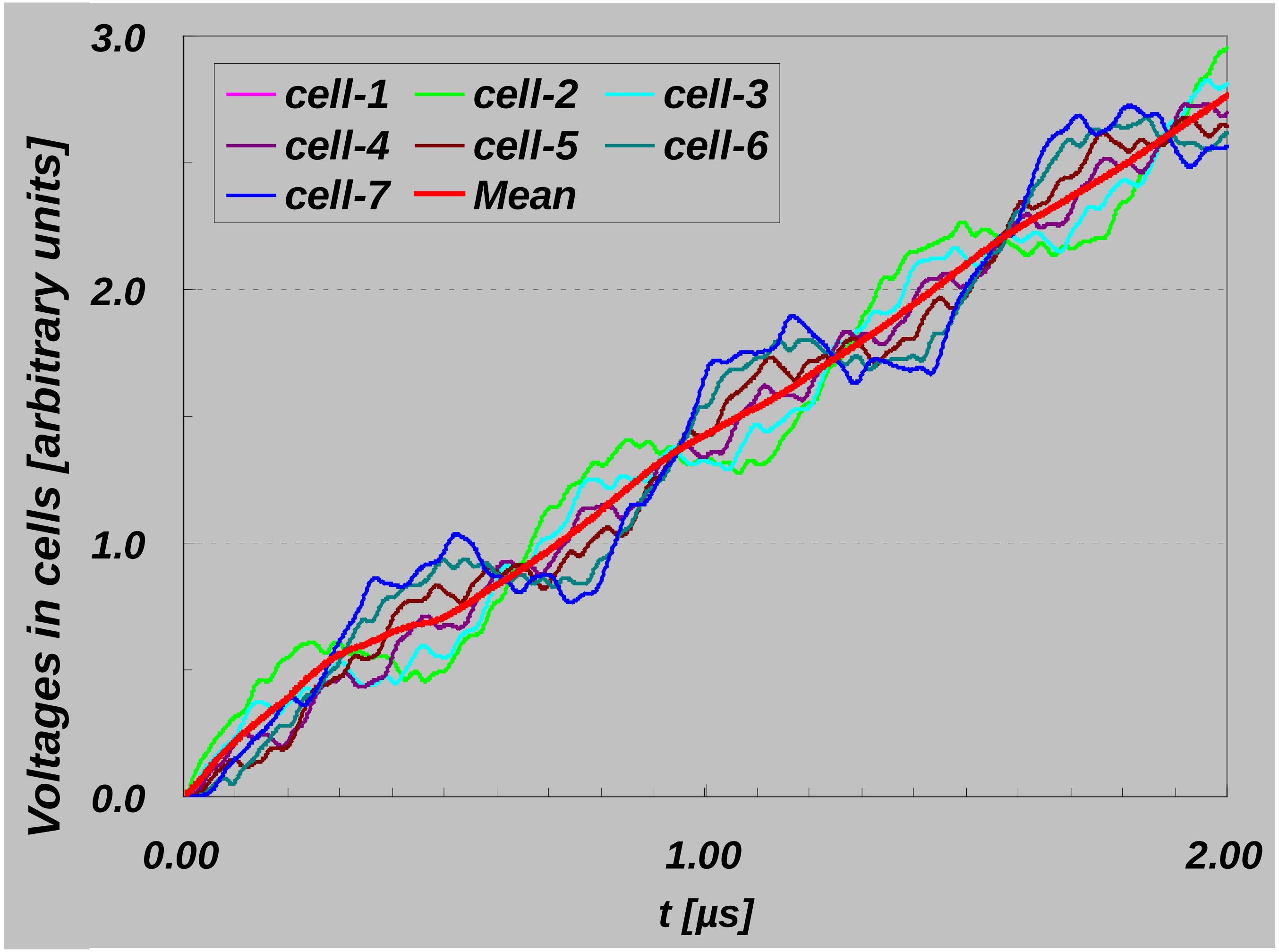

Modeling of the transient state (mode beating at the beam arrival time)

Example: 9-cell TESLA structure, k_{cc}=1.85%, Q_L=3.8 10^6

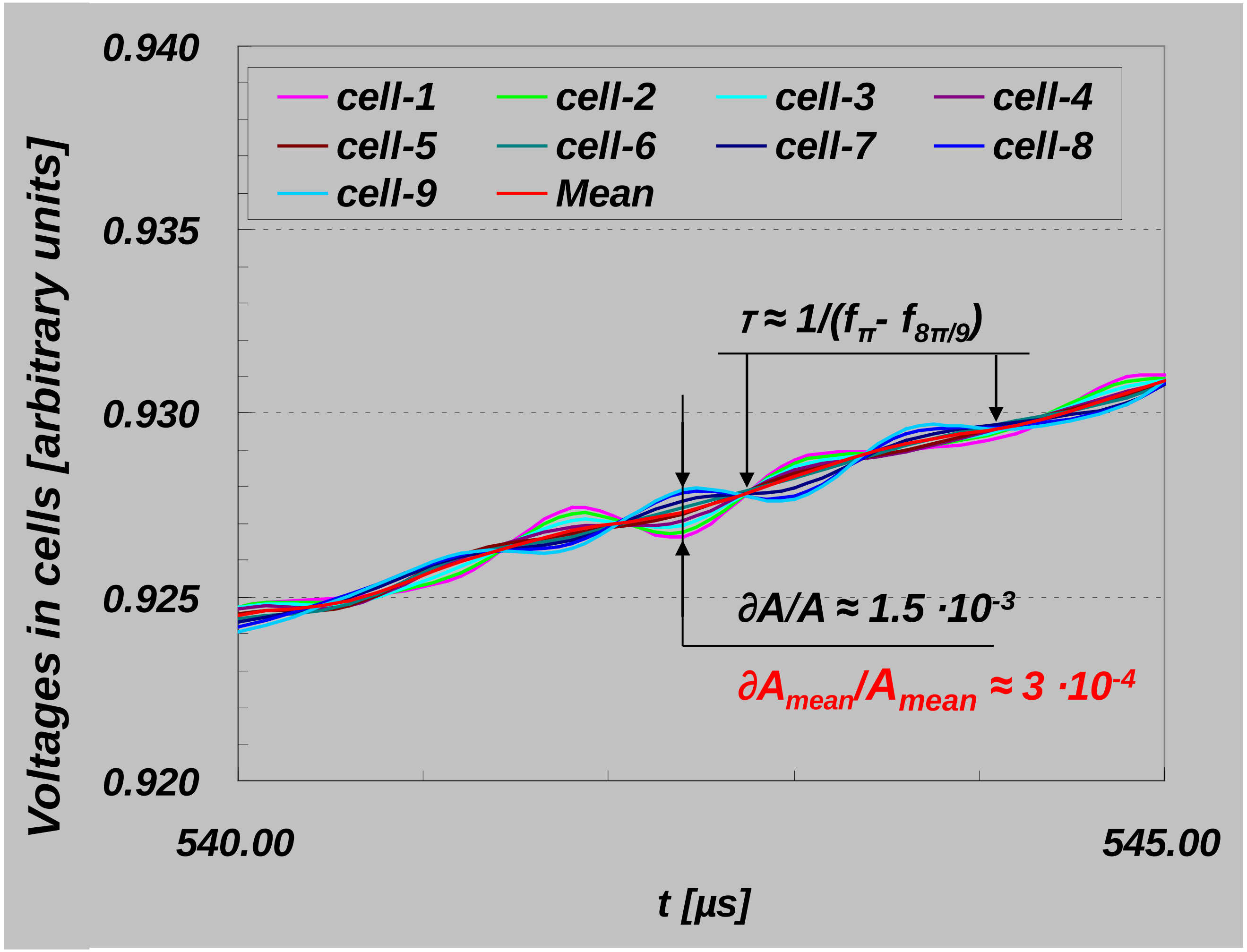

8. Performance test

"Vertical test" at T<Tc (usually ≤ 2K)

The goal is: Q_o vs. E_{acc} (E_{peak})

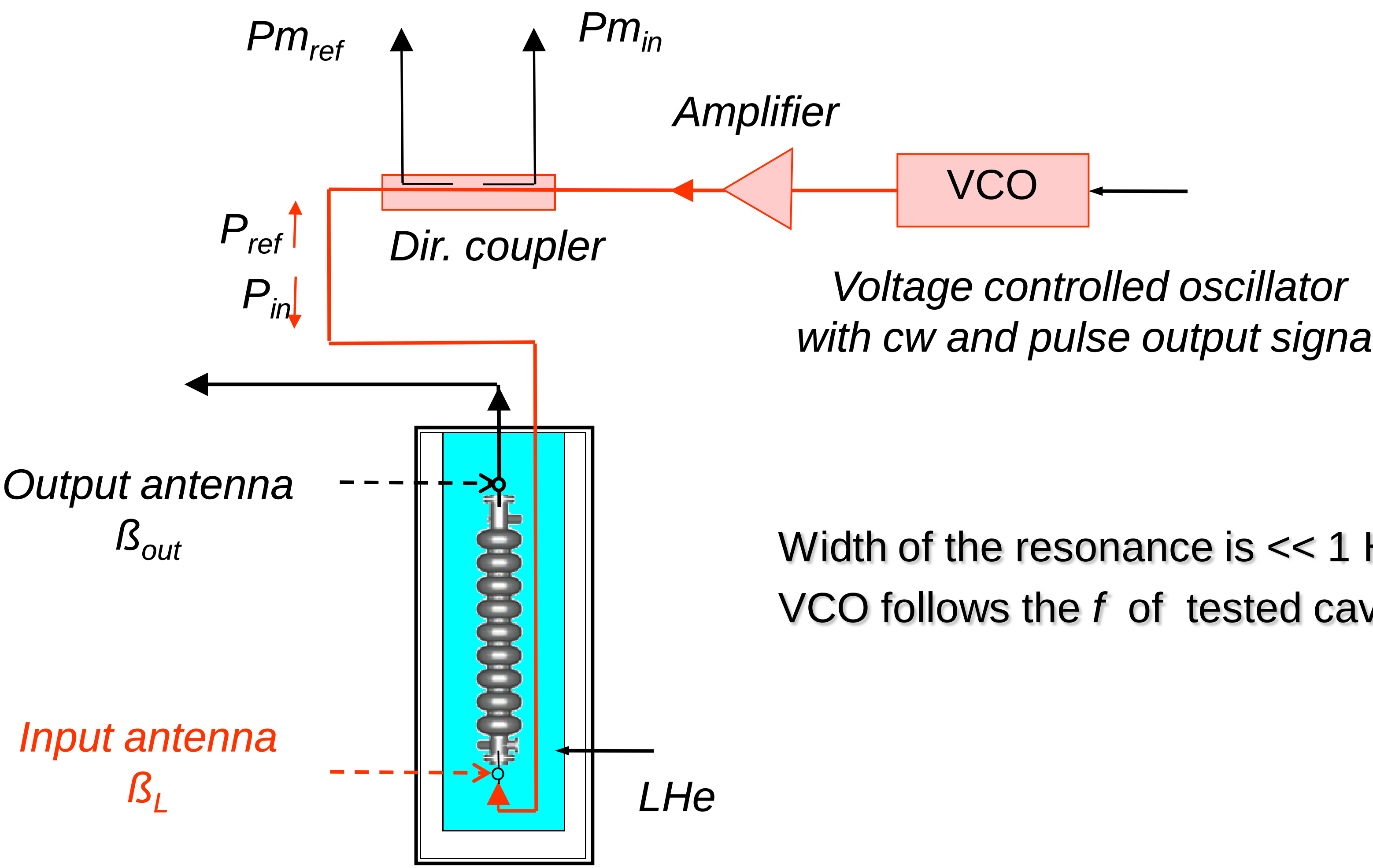

Width of the resonance is << 1 Hz,
VCO follows the *f* of tested cavity

At first, in these tests one measures the coupling strength $ß_L$ and $ß_{out}$ of the input and output antennae.

$$ß_L = \frac{Q_0}{Q_{ext,input}} \qquad ß_{out} = \frac{Q_0}{Q_{ext,output}} \qquad Q_{ext,input} << Q_{ext,output}$$

Step 1.

Cavity response (shape of the reflected wave amplitude) to the rectangular RF-pulse

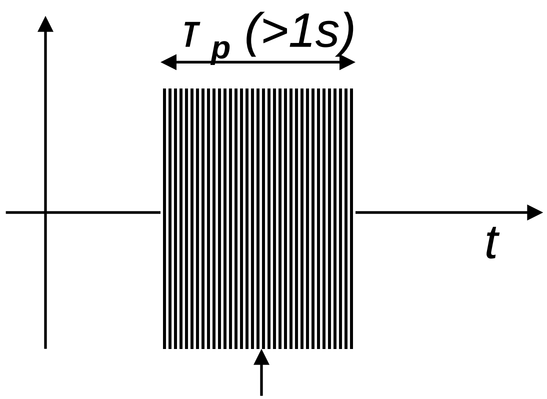

~10^9 RF oscillations at the resonant frequency

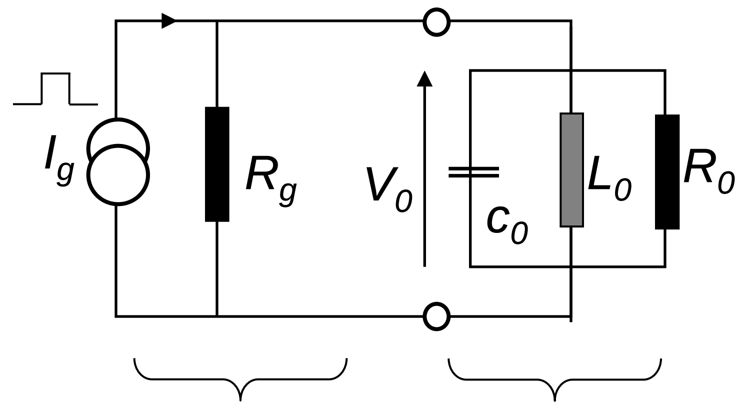

Replacement LEC for the RF-source

Replacement LEC for the tested cavity

$$\begin{cases} f1(t) = -\dfrac{1-\beta_L}{1+\beta_L} - \dfrac{2\beta_L}{1+\beta_L} e^{-\frac{\omega_0 t}{2Q_L}} S(t) & \text{for} \quad t \in <0, \tau_p-> \\ f2(t) = f1(t) + f1(t-\tau_p) S(t-\tau_p) & \text{for} \quad t \in <\tau_p, \infty> \end{cases}$$

where S(t) is the step function.

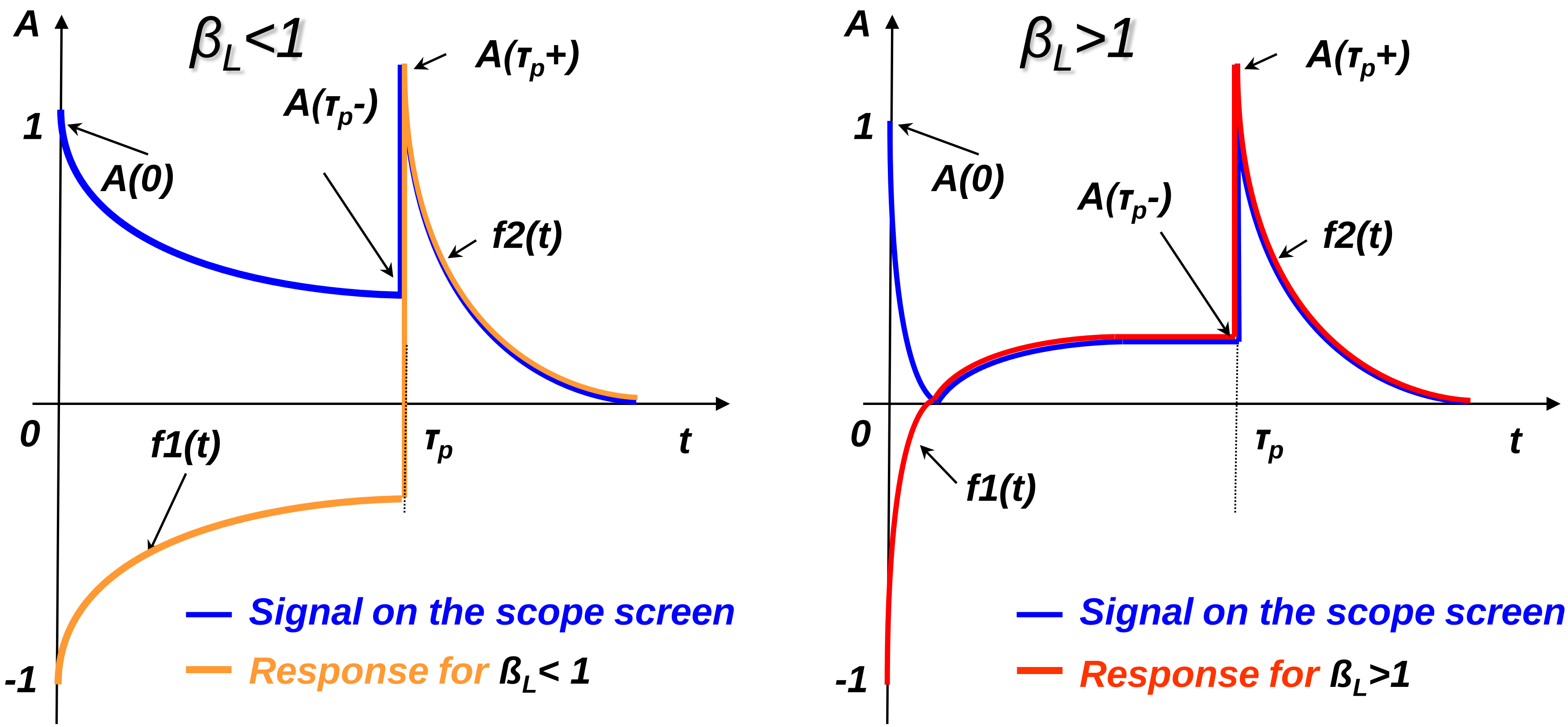

$ß_L$ can be computed with one of the there following formulas:

$$ß_L = \frac{A(0) - A(\tau_p -)}{A(0) + A(\tau_p -)} \qquad ß_L = \frac{A(\tau_p +)}{2A(0) - A(\tau_p +)} \qquad ß_L = \frac{A(\tau_p +)}{2A(\tau_p -) + A(\tau_p +)}$$

Step 2. Energy decay right after the RF-pulse is switched off

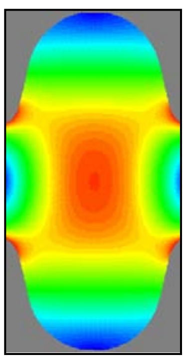

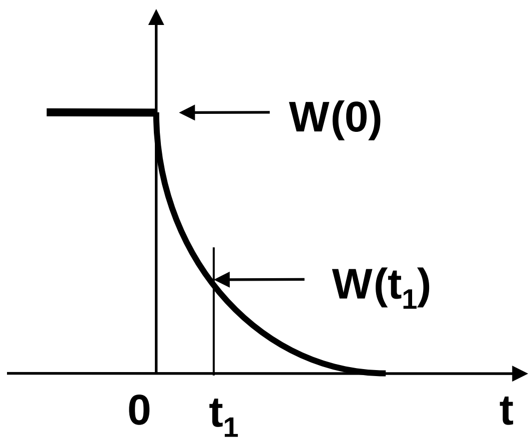

$$W(t) = W(\tau_p +) e^{-\frac{\omega_0 (t - \tau_p +)}{Q_L}}$$

and measuring the input and transmitted power (P_{in} and P_{tran}), one obtains:

$$Q_0 = Q_L (1 + ß_L)(1 + \frac{P_{tran}}{P_{in} - P_{tran}})$$

The mechanical design of a cavity follows its RF design:

- Lorentz Force Detuning
- Mechanical Resonances

Lorentz Force Detuning

$$P = \frac{\mu_0 H_s^2 - \varepsilon_0 E_s^2}{4}$$

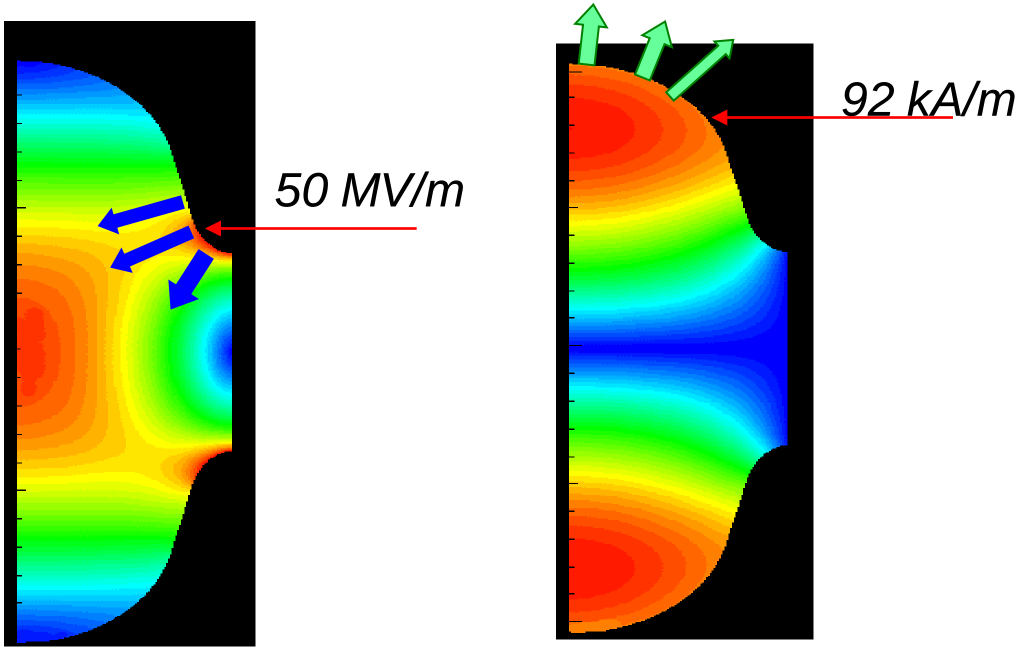

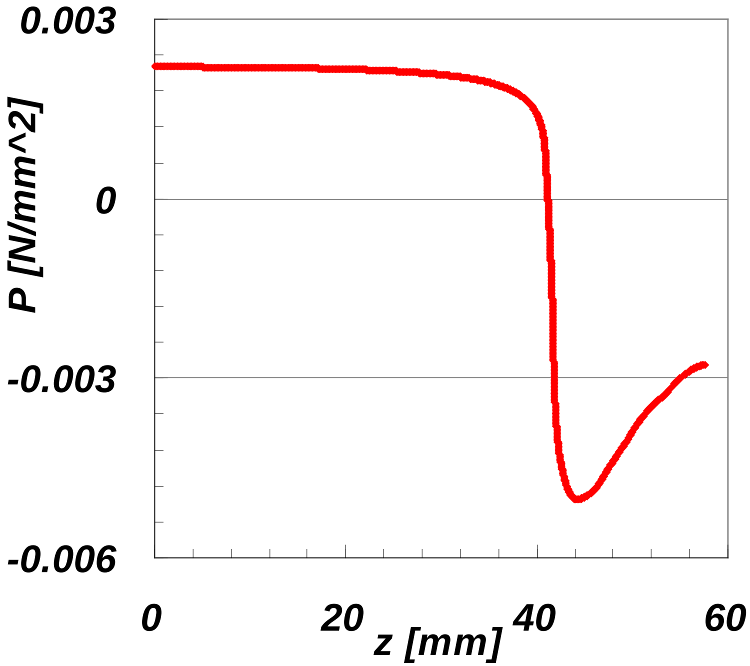

E and H at E_{acc} = 25 MV/m in TESLA inner-cup

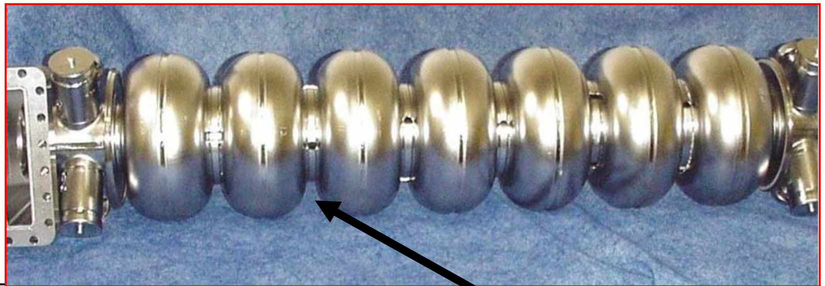

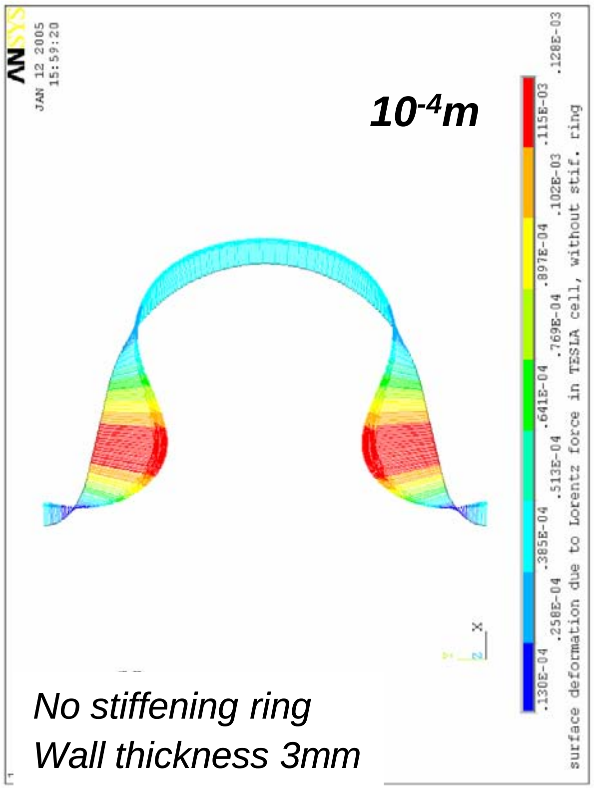

Surface deformation without and with stiffening ring (courtesy of I. Bonin, FERMI)

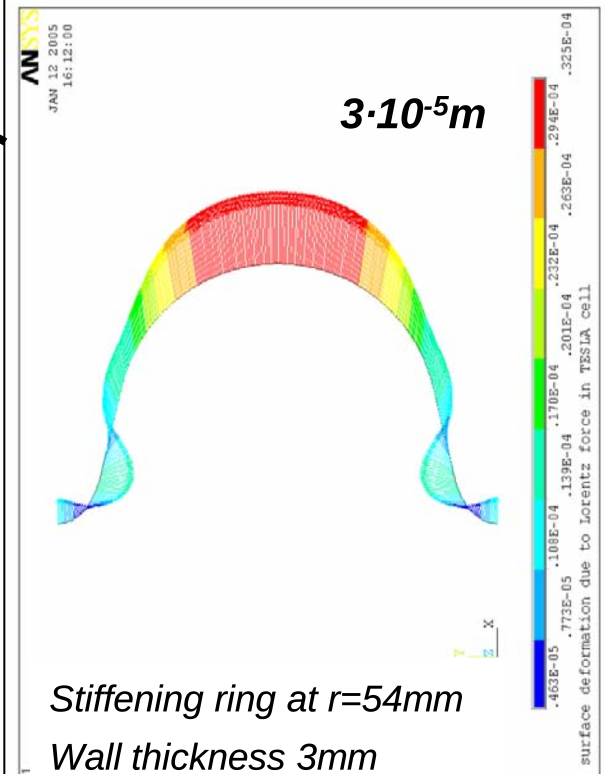

Essential for the operation of a pulsed accelerator $\Delta f = k_L(E_{acc})^2$ $\quad k_L = -1\ Hz/(MV/m)^2$

Mechanical Resonances of a multi-cell cavity

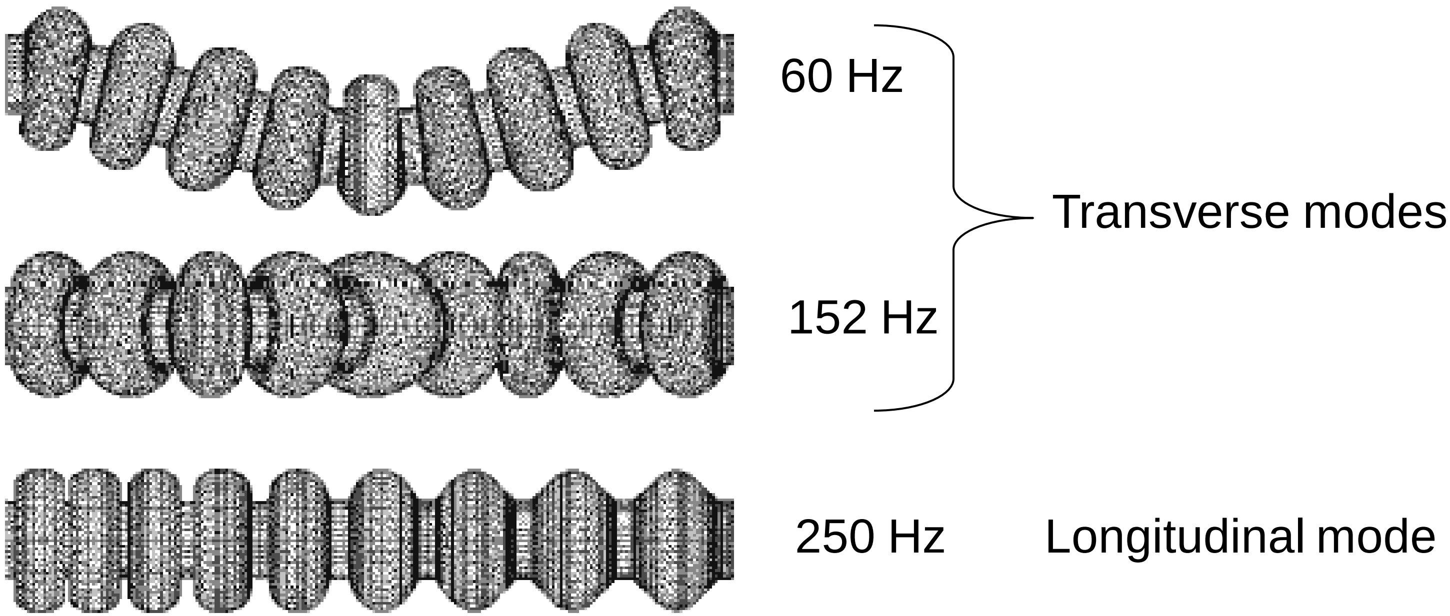

TESLA structure

The mechanical resonances modulate frequency of the accelerating mode.
Sources of their excitation: vacuum pumps, ground vibrations…

The mechanical resonances modulate frequency of the accelerating mode.
Sources of their excitation: vacuum pumps, ground vibrations…

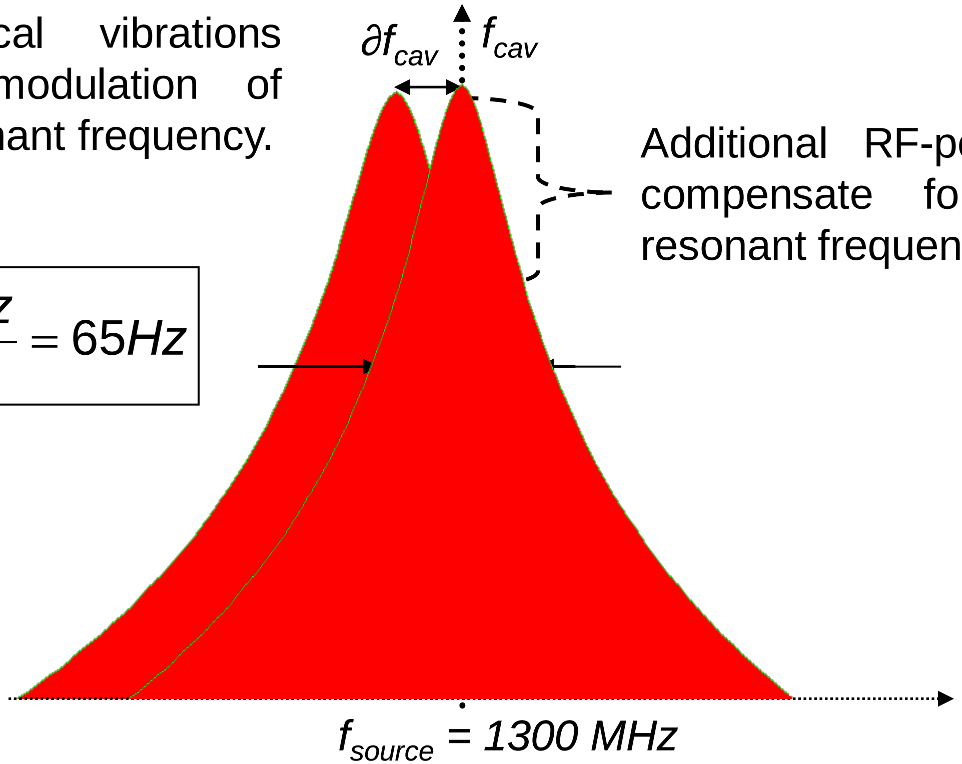

Mechanical vibrations cause modulation of the resonant frequency.

Additional RF-power needed to compensate for the shift of resonant frequency from 1.3GHz.

$$\Delta f_{3db} \equiv \frac{1.3 \cdot 10^{9} Hz}{2 \cdot 10^{7}} = 65 Hz$$

Bibliography

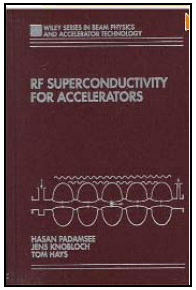

1. H. Padamsee, J. Knobloch, T. Hays, *"RF-Superconductivity for Accelerators"*, Wiley Series in Beam Physics and Accelerator Technology, 1998.

2. Proceedings of all SRF Workshops; http://accelconf.web.cern.ch/accelconf/

3. TESLA TDR, DESY-Report 2003

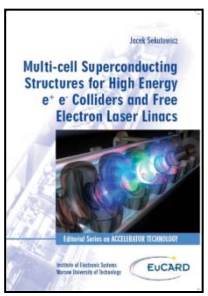

4. J.S. *"Multi-cell Superconducting Structures for High Energy e^+e^- colliders and Free electron Laser Linacs"*, CERN/FP7; http://eucard.web.cern.ch/eucard/